Animal Nutrition 19 (2024) 339–354

Contents lists available at ScienceDirect

Animal Nutrition

journal homepage: http://www.keaipublishing.com/en/journals/aninu/

Original Research Article

A new insight on alleviating the inhibitory effect of aflatoxin B1 on muscle development in grass carp (*Ctenopharyngodon idella*): The effect of 4-Methylesculetin in vivo and in vitro

Xiangning He [a, †], Jiajia Zhang [a, †], Weidan Jiang [a, b, c], Pei Wu [a, b, c], Yang Liu [a, b, c], Hongmei Ren [a], Xiaowan Jin [a], Hequn Shi [d], Xiaoqiu Zhou [a, b, c, *], Lin Feng [a, b, c, *]

[a] *Animal Nutrition Institute, Sichuan Agricultural University, Chengdu 611130, China*
[b] *Fish Nutrition and Safety Production, University Key Laboratory of Sichuan Province, Sichuan Agricultural University, Chengdu 611130, China*
[c] *Key Laboratory for Animal Disease-Resistance Nutrition, Ministry of Education, Ministry of Agriculture and Rural Affairs, Key Laboratory of Sichuan Provence, Chengdu 611130, China*
[d] *Guangzh Cohoo Biotechnology Co., Ltd., Guangzhou 510663, China*

ARTICLE INFO

Article history:
Received 1 May 2024
Received in revised form
1 August 2024
Accepted 18 August 2024
Available online 28 August 2024

Keywords:
4-Methylesculetin
Aflatoxin B1
Muscle development
Grass carp

ABSTRACT

Aflatoxin B1 (AFB1), an important fungal toxin, exists mainly in plant feed ingredients and animals consuming feed contaminated with AFB1 will have reduced growth and impaired health condition mainly due to oxidative stress and reduced immunity. Our previous study found that AFB1 caused oxidative damage and inhibited muscle development of zebrafish. 4-Methylesculetin (4-ME), a coumarin derivative, is now used in biochemistry and medicine widely because of its antioxidant function. Whether 4-ME could alleviate the inhibition of muscle development in grass carp induced by AFB1 has not been reported. In this experiment, 720 healthy grass carp (11.40 ± 0.01 g) were randomly divided into 4 groups with 3 replicates of 60 fish each, including control group, AFB1 group (60 μg/kg diet AFB1), 4-ME group (10 mg/kg diet 4-ME), and AFB1+4-ME group (60 μg/kg diet AFB1 + 10 mg/kg 4-ME diet), for a 60-d growth experiment. In vitro, we also set up 4 treatment groups for grass carp primary myoblast, including control group, AFB1 group (15 μmol/L AFB1), 4-ME group (0.5 μmol/L 4-ME) and AFB1+4-ME group (15 μmol/L AFB1+0.5 μmol/L 4-ME). The results showed that dietary AFB1 decreased growth performance of grass carp, damaged the ultrastructure and induced oxidative damage in grass carp muscle, and significantly decreased the mRNA and protein expression levels of myogenin (MyoG), myogenic differentiation (MyoD), myosin heavy chain (MYHC), as well as the protein expression levels of laminin β1, fibronectin and collagen I ($P < 0.05$), significantly activated the protein expression levels of urokinase-type plasminogen activator (uPA), matrix metalloproteinase-2 (MMP-2), matrix metalloproteinase-9 (MMP-9) and phosphorylate-38 mitogen-activated protein kinase (p38 MAPK) both in grass carp muscle and grass carp primary myoblast ($P < 0.05$). Supplementation of AFB1 with 4-ME significantly improved the growth performance inhibition and alleviated the muscle fiber development inhibition and extracellular matrix (ECM) degradation in grass carp induced by AFB1 ($P < 0.05$). The present results revealed that supplementation of AFB1 contaminated feed with 4-ME reduced the inhibition of growth and muscle development by alleviating AFB1-induced ECM degradation in grass carp,

* Corresponding authors.
E-mail addresses: fishnutrition@126.com (X. Zhou), fenglin@sicau.edu.cn (L. Feng).
† Theses authors contributed to this work equally.
Peer review under the responsibility of Chinese Association of Animal Science and Veterinary Medicine.

Production and Hosting by Elsevier on behalf of KeAi

https://doi.org/10.1016/j.aninu.2024.08.001

which might be related to the p38 MAPK/uPA/MMP/ECM pathway. The results implied that 4-ME could be used as a valuable mycotoxin scavenger in animal feed.

1. Introduction

Aflatoxin B1 (AFB1) is produced mostly by *Aspergillus flavus* and *Aspergillus parasiticus*, which is commonly found in food and animal feed (Chrouda et al., 2020). A considerable portion of fish feed ingredients are derived from commodities (e.g., cereals) that have been found to contain mycotoxins, particularly aflatoxin, deoxynivalenol and fumonisin (Chrouda et al., 2020). Previous findings displayed that AFB1 decreased the growth performance of grass carp (Zeng et al., 2018), induced hepatotoxicity, teratogenicity, and immunosuppression in Nile tilapia (*Oreochromis niloticus*) (Abdelhiee et al., 2021; Hassaan et al., 2020). Furthermore, previous study found that AFB1 inhibited zebrafish muscle development (He et al., 2023a). AFB1 has become one of the most important factors restricting the development of the aquaculture industry. Therefore, it is important to find ways to reduce AFB1 toxicity in feed. Although it has been reported that physical methods (Eshelli et al., 2015), microbial methods (El-Nezami et al., 1998; Lillehoj et al., 1971) and chemical methods (Lillehoj et al., 1971; Yu et al., 2020) could effectively reduce AFB1 toxicity in feed, their application in actual production is limited due to lower efficacy and higher cost.

4-Methylesculetin (4-ME, 6,7-dihydroxy-4-methylcoumarin, formula: $C_{10}H_8O_4$), a coumarin derivative, displays great anti-inflammatory and antioxidant activities (Witaicenis et al., 2018). It was reported that 4-ME increased the activities of glutathione reductase (GR), glutathione peroxidase (GPx), glutathione-S-transferase (GST), and total glutathione (GSH) content in rat colon (Tanimoto et al., 2020). Our previous study found that AFB1 decreased the activities of catalase (CAT) and GST resulting in oxidative damage and inhibition of muscle development in zebrafish (He et al., 2023a). Coumarins, on the other hand, attenuated dexamethasone-induced muscle atrophy (Hah et al., 2023). Therefore, we speculated that 4-ME might alleviate the oxidative damage and the inhibition of muscle development induced by AFB1 in fish. However, there are no relevant studies on whether 4-ME could alleviate the toxicity of mycotoxins and thus necessitates further investigation.

Fish flesh is an important edible protein for humans (Yang et al., 2022). Muscle growth directly affects the flesh quality (Chen et al., 2019). In fish, growth performance is mostly reflected in white muscle growth (Kwasek et al., 2021). Muscle growth and development are complex biological processes controlled by myogenic regulatory factors (MRF) (Hu et al., 2019b). A family of MRF, myogenic differentiation (MyoD), myogenic factor 5 (Myf5), myogenic factor 4 (MRF4), and myogenin (MyoG), regulate the differentiation and determination of myogenesis (Hu et al., 2023). MyoD and Myf5 control stem cells (SC) proliferation (Dong et al., 2022). Furthermore, the *MyoG* gene is a downstream target of the *MRF4* and *MyoD* gene regulatory network, which is necessary for muscle differentiation (Mousavi et al., 2013). The synergistic effect of MRF induces the differentiation of myoblasts into multinucleated muscle tubes (Tiago et al., 2021). Muscle development is also regulated by the extracellular matrix (ECM) (Zhang et al., 2021a). The main components of ECM (collagen, laminin, fibronectin, etc.) are essential for cell attachment, survival, and growth (Bailey et al., 2019). It was reported that collagen I could promote migration and myogenic differentiation of C2C12 (Liu et al., 2020), and laminin could promote proliferation and differentiation of porcine primary muscle cells (Wilschut et al., 2010). Matrix metalloproteinases (MMP) play a crucial role in the cleavage of muscle-specific proteins and the remodeling of the ECM during skeletal muscle growth (Zamanian et al., 2017). A previous study found that AFB1 could activate phosphorylate-38 mitogen-activated protein kinase (p38MAPK) in grass carp spleen (Zeng et al., 2018) and p38MAPK regulated urokinase-type plasminogen activator (uPA, a serine protease) in human umbilical vein endothelial cell line (HUVEC) (Ye et al., 2016). Furthermore, uPA could activate MMP in myeloma cell (Fux et al., 2009). Therefore, we speculated that AFB1 might degrade ECM by activating p38MAPK, and ultimately inhibit muscle development of grass carp. A study on mouse bone marrow cell found that coumarin derivative inhibited p38MAPK activation (Abdallah et al., 2019). So we speculated that 4-ME might alleviate muscle development of grass carp by inhibiting AFB1-induced p38MAPK activation, but the specific mechanism needs to be further explored.

Grass carp (*Ctenopharyngodon idella*) is the world's largest fresh water economic fish and one of the four major Chinese carps (Tang et al., 2019). In this study, grass carp was used to explore the influence of 4-ME alleviating AFB1 on muscle development in vivo. The primary myoblast of grass carp was used to explore the possible mechanism in vitro. The study could provide some theoretical support for the application of 4-ME in fish.

2. Materials and methods

2.1. Animal ethics statement

This study was approved by the Sichuan Agricultural University Animal Care Advisory Committee, and the protocols were approved by the license (HXN2020114011).

2.2. Materials

4-ME (529–84–0) was purchased from Med Chem Exepress (Shanghai, China). AFB1 (purity >98%, 1162–65–8) was provided by Sigma (Aldrich, USA). CCK8 kit (G021-1-1) was obtained from Nanjing Jiancheng Bioengineering Institute (Nanjing, China). Beyotime Biotechnology (Shanghai, China) provided a lactate dehydrogenase (LDH; C0018S) kit. Solaibao (Beijing, China) provided dichloro-dihydro-fluorescein diacetate (DCFH-DA,; CA1410) and 0.25% trypsin–EDTA (2306001). Medium 199 basic (6124119), antibiotic-antimycotic (15240–062), fetal bovine serum (FBS; 2497114P), DMEM/F12 medium (8122172) and goat serum (16210–064) were purchased from Gibco (USA). The environmentally friendly GD fixing solution (G1111) was obtained from Servicebio (Wuhan, China). p38 MAPK inhibitor (SB203580) was obtained from Selleck (Shanghai, China). Malondialdehyde (MDA, A003-1-1), protein carbonyl (PC, A087-1-2), reactive oxygen species (ROS, E–4-1-1) and GST (A004-1-1) kits were obtained from Nanjing Jiancheng Bioengineering Institute (Nanjing, China). Reverse Transcription Kit (RR901A) and Qubit 2.0 Fluorometer (RR047A) were purchased from TaKaRa (Tokyo, Japan). The RNA

extraction kit (RE-03011) was bought from Foregene (Chengdu, China). Trizol kit (R401–01), SYBR Green PCR Kit (Q111–02) was obtained from Novizan Co., Ltd. (Nanjing, China). The enhanced chemiluminescence (ECL) reagent (724D281) was purchased from Oriscience (Chengdu, China).

2.3. Animals

In order to adapt to the situation, the grass carp (purchased from a Sichuan fishery) were pre-fed for 28 d. A total of 720 healthy grass carp with an initial body weight of 11.40 ± 0.01 g were randomly divided into 4 treatments with 3 replicates of 60 fish each. The experimental period was 60 d. There were no dead fish during the whole experiment. The water quality met the basic requirements of fish survival (water temperature was 28.5 ± 2.0 °C, pH was 7.5 ± 0.3, oxygen content > 6.0 mg/L).

2.4. Feeds and experimental design

Composition and nutrient levels of the diet are similar with our previous study (He et al., 2024b), which presented in Table S1. In brief, fish meal, gelatin, and casein were used as major protein sources, and soybean oil and fish oil were used as primary lipid sources. AFB1 was thoroughly mixed with corn starch and this mixture was mixed with other raw materials with fish oil and soybean oil as final additions in the mixture for granulation. The current experiment consisted of four treatment groups: control group, AFB1 group (60 μg/kg diet AFB1), 4-ME group (10 mg/kg diet 4-ME), and AFB1 + 4-ME group (60 μg/kg diet AFB1 + 10 mg/kg diet 4-ME). The fish were fed 4 times a day. After each feeding, the tray was lifted to collect the remaining feed, and weighed them after drying. Feed intake (FI) was calculated as the amount of feed added minus the amount of leftover feed. There were 3 replicates per treatment, and the initial weight and final weight data were obtained by weighing the fish in each replicate group. Six fish was randomly selected from each group to measure their body length.

2.5. Statistics of growth performance

The specific growth rate (SGR), percent weight gain (PWG) and feed efficiency (FE) were calculated according to the initial body weight (IBW), final body weight (FBW) and FI of grass carp, with the following formulae:

$$PWG\ (\%) = 100 \times [FBW\ (g/fish) - IBW\ (g/fish)]/IBW\ (g/fish);$$

$$SGR\ (\%/d) = 100 \times \ln [FBW\ (g)/IBW\ (g)]/days;$$

$$FE\ (\%) = 100 \times [FBW\ (g/fish) - IBW\ (g/fish)]/FI\ (g/fish);$$

$$FI\ (g) = [total\ feed\ (g) - total\ residual\ feed\ quantity\ (g)]/number\ of\ fish\ per\ cage.$$

2.6. Sample collection

After the experiment, the fish were fasted for 24 h, then anaesthetized with benzocaine (50 mg/L). The white muscle was collected from the back of grass carp on ice for further analysis. The diagram of the muscle collection site is displayed in Fig. S1. The part of the muscle was isolated and immediately fixed in GD fixing solution for histological observation. Small pieces of muscle samples were fixed in buffered 2.5% glutaraldehyde for electron microscopic examination. The other muscle samples were stored at −20 or −80 °C for subsequent analyses.

2.7. Cell culture

The grass carp was immersed in 75% alcohol for 3 min. The scales and skin were removed from dorsal and ventral sides, washed white muscle twice in PBS, and then transferred to DMEM/F12 basal medium for cleaning. Then the muscle was cut into pieces with surgical scissors and washed with DMEM/F12 base medium until the medium was clarified. Subsequently, the tissue block was placed in a T25 culture flask and finally in a CO_2 incubator at 28 °C for cell culture. When the tissue blocks were fully attached to the wall, the DMEM/F12 base medium was replaced with M199 complete medium (containing 1% antibiotic-antimycotic and 10% FBS). After a large number of myoblasts were freed from the muscle tissue mass, the cells were partially digested with 0.25% trypsin before sub-culturing. In this experiment, fibroblasts were removed using the differential velocity adherent method three times (20 min each time), and then the supernatant and seed were kept in a T25 culture flask for culture of grass carp primary myoblasts.

2.8. AFB1 treatment and SB203580 treatment

When the density of the grass carp primary myoblasts reached about 80%, the cell suspension was collected after digestion with 0.25% trypsin and spread on the cell culture plate. When the cells reached 80% of the well area, the cells were treated with M199 complete medium (control group), M199 complete medium containing 15 μmol/L AFB1 (AFB1 group), M199 complete medium containing 0.5 μmol/L 4-ME (4-ME group) and M199 complete medium containing 15 μmol/L AFB1 + 0.5 μmol/L 4-ME (AFB1 + 4-ME group) for 24 h. The dose of AFB1 was determined according to our preliminary experimental results (He et al., 2024a), and the dose of 4-ME was determined through pre-experimental screening. Afterward, cells were collected for experimental analysis.

For SB203580 treatment, the grass carp primary myoblasts were preincubated with or without p38 inhibitor (SB203580) for 1 h, then treated with or without AFB1 or 4-ME for 24 h. The groups and treatments were: control group (without SB203580 pre-treatment or AFB1 or 4-ME), AFB1 group (with 15 μmol/L AFB1 treatment for 24 h), SB203580 group (with 10 μmol/L SB203580 pre-treatment for 1 h), AFB1 + 4-ME group (with 15 μmol/L AFB1 and 0.5 μmol/L 4-ME treatment for 24 h), AFB1 + SB203580 group (with 10 μmol/L SB203580 pre-treatment for 1 h, followed by 15 μmol/L AFB1 treatment for 24 h), AFB1 + 4-ME + SB203580 group (with 10 μmol/L SB203580 pre-treatment for 1 h, followed by 15 μmol/L AFB1 and 0.5 μmol/L 4-ME treatment for 24 h). The dose of SB203580 was determined according to our pre-experimental and previous study (He et al., 2024a). Furthermore, 10 μmol/L SB203580 had a significant effect on C2C12 cells (Kumar and Dey, 2002). Therefore, in this experiment, the effective dose of SB203580 was selected at 10 μmol/L. For further examination, cells were collected following relevant treatments.

2.9. Cell viability assay

In this study, the cell viability was measured using a CCK8 kit. In brief, in 96-well plates, the growth of cells to 80% confluence was followed by two PBS washes and 24 h of incubation in M199 complete medium with or without AFB1 or 4-ME. Afterward, 10 μL

CCK8 was added into 96-well plates, incubated with cells for 2 h. Using a microplate spectrophotometer, absorbance at 450 nm was measured for quantification.

2.10. LDH release assay

In this study, LDH release was detected using the LDH Cytotoxicity Detection Kit. In brief, cells were treated with 150 μL of LDH release reagent, collected 120 μL of supernatants from each well, and then analyzed them using a microplate reader. After mixing the working fluid with the supernatant at 490 nm, the absorbance was measured after incubation at room temperature for 30 min.

2.11. Detection of ROS levels

After centrifugation (1000 × *g*, 5 min) and digestion with 0.25% trypsin, cells were collected. The DCFH-DA fluorescence probe was diluted 1:1000 in a serum-free medium. The myoblast was incubated with a DCFH-DA fluorescence probe for 30 min in the dark. Finally, the ROS levels were detected by a flow cytometer (CytoFlex, Beckman Coulter, Inc., USA).

2.12. Histological observation

The collagen in the muscle was stained with sirius red, deparaffinized 4 μm sections with xylene and hydrated them in graded alcohols. The sections were then stained with sirius red for 5 min and then rinsed in distilled water. Finally, the section was dehydrated and the tablet was sealed. An oven-dried sample was examined under a microscope (TS100, Nikon, Tokyo, Japan). The area of collagen fiber was counted by Image J.

2.13. Transmission electron microscopy (TEM) observation

The muscle samples were fixed in glutaraldehyde for 24 h followed by osmium tetroxide for 2 h. In all samples, acetone was used for dehydration, epoxy resin (Epon 812) was used for embedding, slices were cut and uranium acetate and lead citrate were used for dyeing. In the end, the sections were observed and photographed under a JEM-1400FLASH transmission electron microscope (JEOL, Tokyo, Japan).

Cell samples were digested using 0.25% trypsin and centrifuged (1000 × *g*, 5 min). The cells were then fixed with electron microscope fixation liquid for 2 h. The procedure of embedding, slicing and dyeing of the sample was the same as that of the muscle sample.

2.14. Biochemical analysis

The biochemical analysis included MDA, PC, ROS and GST and the specific methods of these indicators were carried out according to the instructions. Briefly, a physiologic saline solution with 9 volumes was used to homogenize the muscle samples and the samples were centrifuged for 15 min at 1200 × *g*. The supernatant was collected to detect biochemical indicators. The parameters of the kits are shown in Table S2.

2.15. Real-time PCR

For muscle sample preparation, total RNA was extracted using the Trizol kit. The cells were treated with AFB1 or 4-ME for 24 h at 6-well plates. RNA from the cells was extracted from a total RNA extraction kit (RT-01021, Foregene, Chengdu, China). The integrity of RNA was assessed by electrophoresis on agarose gels, and the concentration of RNA was measured by Qubit 2.0 Fluorometer. The RNA was reversed transcribe to cDNA using a Reverse Transcription Kit. A list of primer sequences is provided in Table 1 β-Actin was selected as internal reference gene for these analyses. The extracted DNA was quantified using the SYBR Green PCR Kit. PCR reaction components included 5 μL SYBR Green Premix, l μL cDNA, 3.4 μL DEPC water, 0.2 μL ROX, 0.2 μL forward primers and 0.2 μL reverse primers. The PCR reaction procedure was as follows: 95 °C for 30 s, followed by 95 °C for 15 s and 60 °C for 34 s, then 95 °C for 15 s, and finally 60 °C for 1 min and 95 °C for 15 s for 40 cycles using QuantStudio 5 Real-Time PCR System (Thermo Fisher Scientific, Waltham, MA, USA). Based on the $2^{-\Delta\Delta Ct}$ method, gene expression was calculated.

2.16. Immunofluorescence assay

The paraffin-embedded muscle was sectioned and deparaffinized them in xylene before rehydrating in ethanol in decreasing concentrations. The cells were treated with AFB1 or 4-ME for 24 h at 6-well plates. After treatment, the cells were fixed using 4% paraformaldehyde for 20 min, and then permeabilized with 0.2% Triton X-100 for 20 min at room temperature. The samples were then washed in PBS for 5 min followed by 1 h of blocking with 5% BSA and incubation with primary antibody at 4 °C overnight, and secondary antibody for 1 h protected from light. After staining the nucleus with DAPI for 10 min, the images were collected under a fluorescence microscope (Leica, Wetzlar, Germany). Information on the antibodies is displayed in Table S3.

2.17. Western blot assay

Protein was isolated from tissue lysates using RIPA lysis buffer following the extraction of fish muscle. The supernatants of the lysates were collected after centrifugation (12,000 × *g*, 15 min). The protein levels were detected in supernatants using a BCA Protein Assay Kit (Nanjing Jiancheng, China). The isolation of proteins was accomplished through all manipulations conducted on ice. The protein lysates were separated by sodium dodecyl sulfate polyacrylamide gel electrophoresis (SDS-PAGE) and transferred them to polyvinylidene difluoride (PVDF) membranes by electrophoresis. Afterward, a primary antibody solution was incubated overnight on PVDF membranes at 4 °C, followed by incubation with secondary antibodies for 1 h. In the final step of the process, enhanced chemiluminescence (ECL) reagent was used to visualize the blots. The internal reference protein was β-Actin and glyceraldehyde-3-phosphate dehydrogenase (GAPDH). Information on the antibodies is displayed in Table S4. The blotted bands were quantified using Image J.

2.18. Statistical analysis

Data are presented as mean ± standard deviation (mean ± SD). Two-way analysis of variance (ANOVA) was used to compare multiple groups. The significance level was considered to be $P < 0.05$. The data were analyzed by Student's *t*-test using SPSS 27.0 in SB203580 treatment. * indicated $P < 0.05$, ** indicated $P < 0.01$, and *** indicated $P < 0.001$, # indicated $P < 0.05$, ## indicated $P < 0.01$, ns indicated $P > 0.05$, the difference is not significant. With the help of Image J, images were analyzed for quantification. Softwares used for data processing were GraphPad Prism 8 and Home for researchers (www.home-for-researchers.com).

Table 1
Real-time polymerase chain reaction primer sequences.

Item	Primer sequence of forward (5' to 3')	Primer sequence of reverse (5' to 3')	Temperature, °C
MyoD	CCCTTGCTTCAACACCAACG	TCTCCTCTCCCTCATGGTGG	54.0
MyoG	AGAGGAGGTTGAAGAATTTC	GTTCCTGCTGGTTGAGAGA	59.0
MYHC	ACGCTCATCACCACCAACCC	CAGCCTCCTCTGTGCCATCA	60.0
MMP-2	GAGCTGTGGACATTAGGAGAAG	GAACAAGAGCTCATGAGGACAG	60.0
MMP-9	ACTTGGAGTTGTGGCTTTTC	AGGGCTCTGTCATCAGGTTA	60.0
p38 MAPK	GGGAGCAGACCTCAACAA	CCATCGGGTGGCAACATA	61.0
JNK	ACAGCGTAGATGTGGGTGATT	GCTCAAGGTTGTGGTCATACG	62.3
ERK	GGACAGAAACGATGGCGGAA	CCCGTGATGACTGTCCCTCT	56.0
β-Actin	GGCTGTGCTGTCCCTGTA	GGGCATAACCCTCGTAGAT	61.4

MyoD = myogenic differentiation; *MyoG* = myogenin; *MYHC*= myosin heavy chain; *MMP*= matrix metalloproteinases; *p38 MAPK*= p38 mitogen-activated protein kinase; *JNK* = c-Jun N-terminal kinase; *ERK*= extracellular signal-regulated kinase.

3. Results

3.1. 4-ME alleviated the growth performance, muscle ultrastructure and oxidative damage induced by AFB1 in grass carp

The growth of fish directly determined the growth and development of muscle. As shown in Table 2, AFB1 significantly inhibited the FBW, PWG, SGR, FI and FE ($P < 0.05$). However, AFB1 + 4-ME treatment improved the inhibition effects of AFB1 in grass carp ($P < 0.05$). Furthermore, AFB1 damaged the ultrastructure of grass carp muscle, and induced endoplasmic reticulum expands, while AFB1+ 4-ME treatment alleviated the damage to grass carp muscle (Fig. 1). In addition, the MDA, ROS and PC levels were increased significantly ($P < 0.05$), and the GST activity was decreased in grass carp muscle in AFB1 group ($P < 0.001$), but AFB1 + 4-ME treatment alleviated the levels of change in these indicators ($P < 0.05$) (Table 3). These findings demonstrated that 4-ME alleviated the growth performance, muscle ultrastructure and oxidative damage induced by AFB1 in grass carp.

3.2. 4-ME alleviated AFB1-induced decrease in expression of MRF in grass carp muscle

AFB1 significantly down-regulated the relative mRNA expression levels of MRF (including *MyoD*, *MyoG* and *MYHC*) ($P < 0.05$), while AFB1 + 4-ME treatment improved above relative mRNA expression levels in grass carp muscle ($P < 0.05$) (Fig. 2A–C). Furthermore, the effect of AFB1 on relative mRNA expression levels *of MyoD*, *MyoG* and *MYHC* in grass carp muscle was determined by assessing the abundance of MRF protein. AFB1 decreased the protein expression levels and fluorescence intensity of MyoD, MyoG and MYHC ($P < 0.05$), but AFB1 + 4-ME treatment improved the protein expression levels and fluorescence intensity in grass carp muscle (Fig. 2D–I) ($P < 0.05$). The data suggested that 4-ME

Table 2
Growth performance of grass carp for 60 d.

Item	Group[1]				*P*-value			
	Control	AFB1	4-ME	AFB1+4-ME	Treatment	4-ME	AFB1	AFB1+4-ME
IBW, g	11.40 ± 0.010	11.40 ± 0.011	11.40 ± 0.020	11.41 ± 0.001	0.374	0.332	0.620	0.160
FBW, g	167.04 ± 2.160^{b}	135.88 ± 2.632^{a}	232.78 ± 5.141^{d}	188.46 ± 3.073^{c}	<0.001	<0.001	<0.001	0.011
PWG, %	1365.24 ± 18.950^{b}	1091.95 ± 23.114^{a}	1941.96 ± 45.120^{d}	1553.12 ± 26.961^{c}	<0.001	<0.001	<0.001	0.011
SGR, %/d	4.47 ± 0.021^{b}	4.13 ± 0.032^{a}	5.03 ± 0.040^{d}	4.68 ± 0.032^{c}	<0.001	<0.001	<0.001	0.702
FI, g	148.62 ± 0.510^{b}	125.29 ± 0.279^{a}	204.69 ± 0.851^{d}	162.65 ± 1.893^{c}	<0.001	<0.001	<0.001	<0.001
FE, %	1.05 ± 0.013^{b}	0.99 ± 0.021^{a}	1.08 ± 0.022^{bc}	1.09 ± 0.020^{c}	0.002	0.001	0.085	0.033

IBW = initial body weight; FBW = final body weight; PWG = percent weight gain; SGR = specific growth rate; FI = feed intake; FE = feed efficiency.
$^{a-d}$ Different letters represent significant differences ($P < 0.05$).
[1] Control = control group, AFB1 = 60 μg/kg diet AFB1, 4-ME = 10 mg/kg diet 4-ME, AFB1+4-ME = 60 μg/kg diet AFB1 + 10 mg/kg diet 4-ME. The data represent means ± SD.

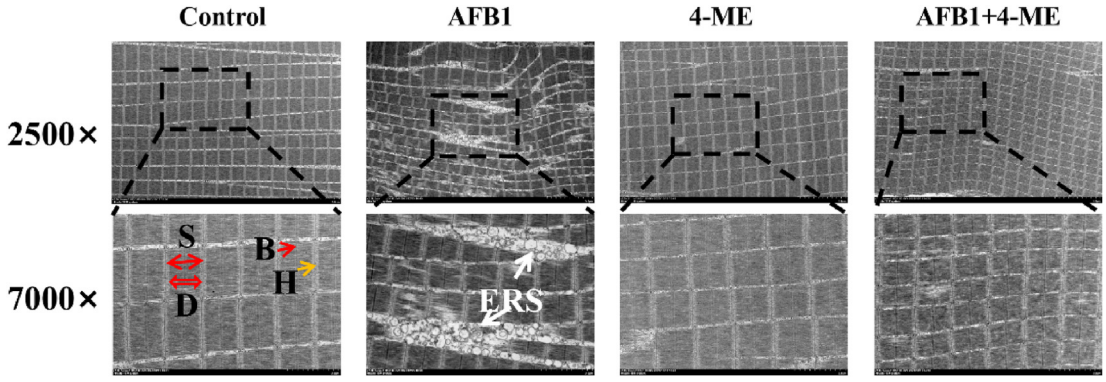

Fig. 1. 4-Methylesculetin (4-ME) alleviated the effects of aflatoxin B1 (AFB1) on muscle ultrastructure of grass carp (captured using a transmission electron microscope). S = sarcomere; D = dark band; B = bright band; H=H band; ERS = endoplasmic reticulum expands. Control = control group; AFB1 = 60 μg/kg diet AFB1; 4-ME = 10 mg/kg diet 4-ME; AFB1+4-ME = 60 μg/kg diet AFB1 + 10 mg/kg diet 4-ME.

Table 3
4-ME alleviated the effects of AFB1 on antioxidant capacity and the contents of collagen of grass carp muscle.

Item	Group[1]				*P*-value			
	Control	AFB1	4-ME	AFB1+4-ME	Treatment	4-ME	AFB1	AFB1+4-ME
ROS, %	100.00 ± 6.331^{b}	120.16 ± 15.670^{c}	79.44 ± 4.215^{a}	92.17 ± 3.898^{b}	<0.001	<0.001	0.002	0.105
MDA, nmol/mg prot	4.91 ± 0.673^{ab}	6.87 ± 0.813^{c}	4.62 ± 0.566^{a}	5.57 ± 0.536^{b}	<0.001	0.003	<0.001	0.093
PC, nmol/mg prot	5.11 ± 0.645^{ab}	9.10 ± 0.651^{c}	5.71 ± 0.651^{b}	4.44 ± 0.600^{a}	<0.001	<0.001	<0.001	<0.001
GST, U/mg prot	84.33 ± 6.162^{b}	71.60 ± 6.227^{a}	91.58 ± 4.626^{c}	78.91 ± 2.357^{b}	<0.001	0.002	<0.001	0.840
Collagen, μg/mg prot	4.23 ± 0.523^{b}	3.31 ± 0.423^{a}	5.69 ± 1.048^{c}	4.78 ± 0.598^{b}	<0.001	0.001	0.001	0.861

4-ME = 4-Methylesculetin; AFB1 = aflatoxin B1; ROS = reactive oxygen species; MDA = malondialdehyde; PC = protein carbonyl; GST = glutathione-S-transferase.
[a-c] Different letters represent significant differences ($P < 0.05$).
[1] Control = control group, AFB1 = 60 μg/kg diet AFB1, 4-ME = 10 mg/kg diet 4-ME, AFB1+4-ME = 60 μg/kg diet AFB1+ 10 mg/kg diet 4-ME. The data represent means ± SD.

alleviated the inhibition of MRF expression induced by AFB1 in grass carp muscle.

3.3. 4-ME alleviated AFB1-induced decrease of ECM main components expression in grass carp muscle

The development of skeletal muscle is highly complex and sophisticated biological process and is regulated by MRF and ECM main components (including laminin β, fibronectin and collagen I). A sirius red stain showed that collagen I abundance decreased in the AFB1 group ($P < 0.001$), while it was better in AFB1 + 4-ME group ($P < 0.001$) (Fig. 3A and D). The detection of collagen contents showed similar results (Table 3), and the Western blot analysis results were identical to that of sirius red assay (Fig. 3G). Results of immunofluorescence and Western blot revealed that AFB1 decreased the protein expression levels and fluorescence intensity of laminin β1 and fibronectin ($P < 0.05$), while AFB1 + 4-ME treatment improved the expression of these proteins in grass carp muscle (Fig. 3B and C, 3E and F, 3H and I) ($P < 0.05$). These data indicated that 4-ME alleviated the decrease of ECM abundance induced by AFB1 in grass carp muscle.

3.4. 4-ME alleviated the inhibitory effect of AFB1 on muscle development of grass carp mediated by the p38MAPK signaling pathway

To assess the effects of 4-ME alleviating AFB1 on muscle development, further explored the signaling pathway regulating ECM degradation. It was found that the *MMP-2, MMP-9* and *p38 MAPK* relative mRNA expression levels were up-regulated in AFB1 group and these down-regulated following dietary AFB1 + 4-ME treatment (Fig. 4A) ($P < 0.05$). The transcriptional levels of *JNK* and *ERK1* did not change in AFB1 group compared to Control group ($P > 0.05$) (Fig. 4A). Moreover, the Western blot results displayed that AFB1 increased the protein expression levels of p-p38 MAPK/p38 MAPK, uPA, MMP-2 and MMP-9 in grass carp muscle ($P < 0.05$), while AFB1 + 4-ME treatment decreased these proteins expression levels (Fig. 4B) ($P < 0.05$). These results indicated that 4-ME alleviated the inhibitory effect of AFB1 on the muscle development of grass carp, which might be mediated by the p38 MAPK signaling pathway.

3.5. 4-ME alleviated the cell damage and the decrease of cell viability induced by AFB1 in grass carp primary myoblasts

AFB1 treatment increased the death of primary myoblasts of grass carp but AFB1 + 4-ME treatment improved their survival (Fig. 5A). Further observed the ultrastructure of the cells through TEM and the results showed that AFB1 induced mitochondrial swelling, while AFB1 + 4-ME treatment alleviated the cells damage (Fig. 5B). Using flow cytometer measured ROS levels, the findings displayed that ROS levels were significantly improved in AFB1 group ($P < 0.001$), however, AFB1 + 4-ME treatment decreased the ROS levels (Fig. 5C and Table 4) ($P < 0.001$). The results of cell viability and cytotoxicity displayed that AFB1 significantly decreased the viability and increased LDH release of primary myoblasts ($P < 0.05$), while AFB1 + 4-ME treatment effectively alleviated these toxic effects (Table 4) ($P < 0.05$). These observations suggested that 4-ME alleviated the cell damage and cytotoxicity induced by AFB1.

3.6. 4-ME alleviated the decrease of MyoD expression in grass carp primary myoblasts induced by AFB1

To explore the alleviating effect of 4-ME on *MyoD* relative mRNA expression level in grass carp primary myoblasts induced by AFB1, the mRNA expression was firstly detected. The results showed that 4-ME effectively alleviated the down-regulation of *MyoD* transcriptional level induced by AFB1 (Fig. 6A) ($P < 0.001$), and the protein detection also showed the same results (Fig. 6B) ($P < 0.001$). Further detected the abundance of MyoD in grass carp primary myoblasts by immunofluorescence and found that AFB1 + 4-ME treatment significantly improved MyoD expression level compared to AFB1 group (Fig. 6C) ($P < 0.001$). These findings demonstrated that 4-ME alleviated the decreased expression of MyoD induced by AFB1, thereby alleviating the inhibitory effect of AFB1 on myoblast development.

3.7. 4-ME alleviated the decreased expression of ECM main components in grass carp primary myoblasts induced by AFB1

To explore the possible reasons why 4-ME alleviated the inhibition of AFB1 on myoblast development, the expression of ECM main components in myoblasts were examined. As shown in Fig. 7A–D, AFB1 decreased the abundance of collagen I and fibronectin in grass carp primary myoblasts, while AFB1 + 4-ME treatment improved their abundance ($P < 0.05$). Next, the protein expression levels of ECM main components (including collagen I, laminin β1 and fibronectin) were detected. The data displayed that AFB1 significantly decreased the protein expression levels, while AFB1 + 4-ME treatment improved the protein expression levels (Fig. 7E) ($P < 0.05$). These findings suggested that 4-ME alleviated the decreased expression of ECM main components in grass carp primary myoblasts induced by AFB1.

3.8. 4-ME and SB203580 inhibited the activation of p38 MAPK signaling pathway induced by AFB1 in grass carp primary myoblasts

In order to investigate the mechanism by which 4-ME alleviated the inhibition of AFB1-induced myoblast development, the enzyme activity, genes and protein expression of ECM components degradation in myoblasts were examined. The data showed that AFB1

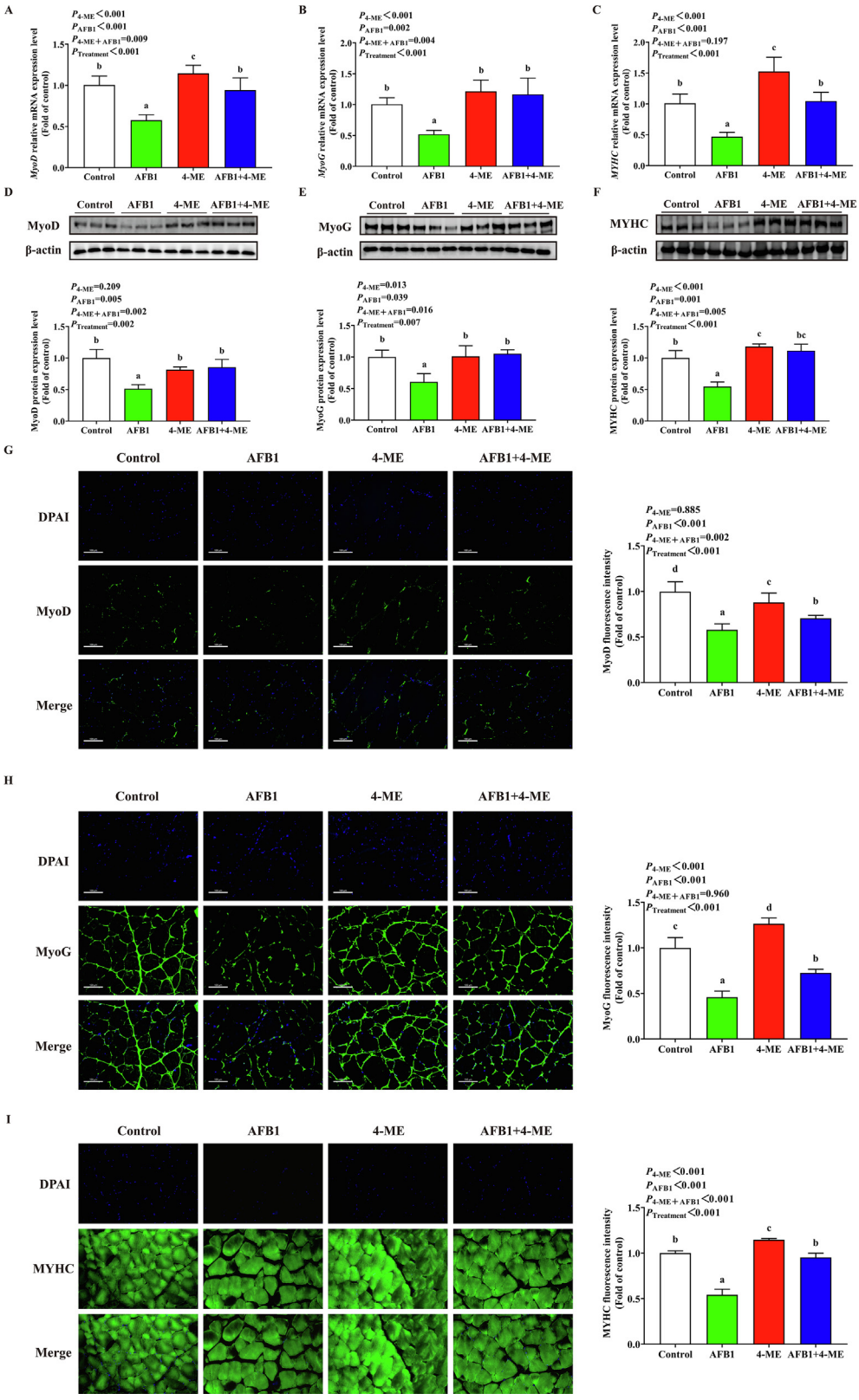

Fig. 2. 4-Methylesculetin (4-ME) alleviated the effects of aflatoxin B1 (AFB1) on the expression of myogenic regulatory factors (MRF) in muscle of grass carp. (A) Relative mRNA expression levels of *MyoD*. (B) Relative mRNA expression levels of *MyoG*. (C) Relative mRNA expression levels of *MYHC*. (D) The protein expression levels of MyoD. (E) The protein expression levels of MyoG. (F) The protein expression levels of MYHC. (G) Representative images of MyoD distribution (200 ×) and fluorescence intensity of MyoD protein expression levels. (H) Representative images of MyoG distribution (200 ×) and fluorescence intensity of MyoG protein expression levels. (I) Representative images of MYHC distribution (200 ×) and fluorescence intensity of MYHC protein expression levels. Control = control group, AFB1 = 60 μg/kg diet AFB1, 4-ME = 10 mg/kg diet 4-ME, AFB1+4-ME = 60 μg/kg diet AFB1 + 10 mg/kg diet4-ME. $^{a\text{-}d}$ Different letters represent significant differences ($P < 0.05$). The data represent means ± SD. MyoD = myogenic differentiation; MyoG = myogenin; MYHC = myosin heavy chain; DPAI = 4',6-diamidino-2-phenylindole.

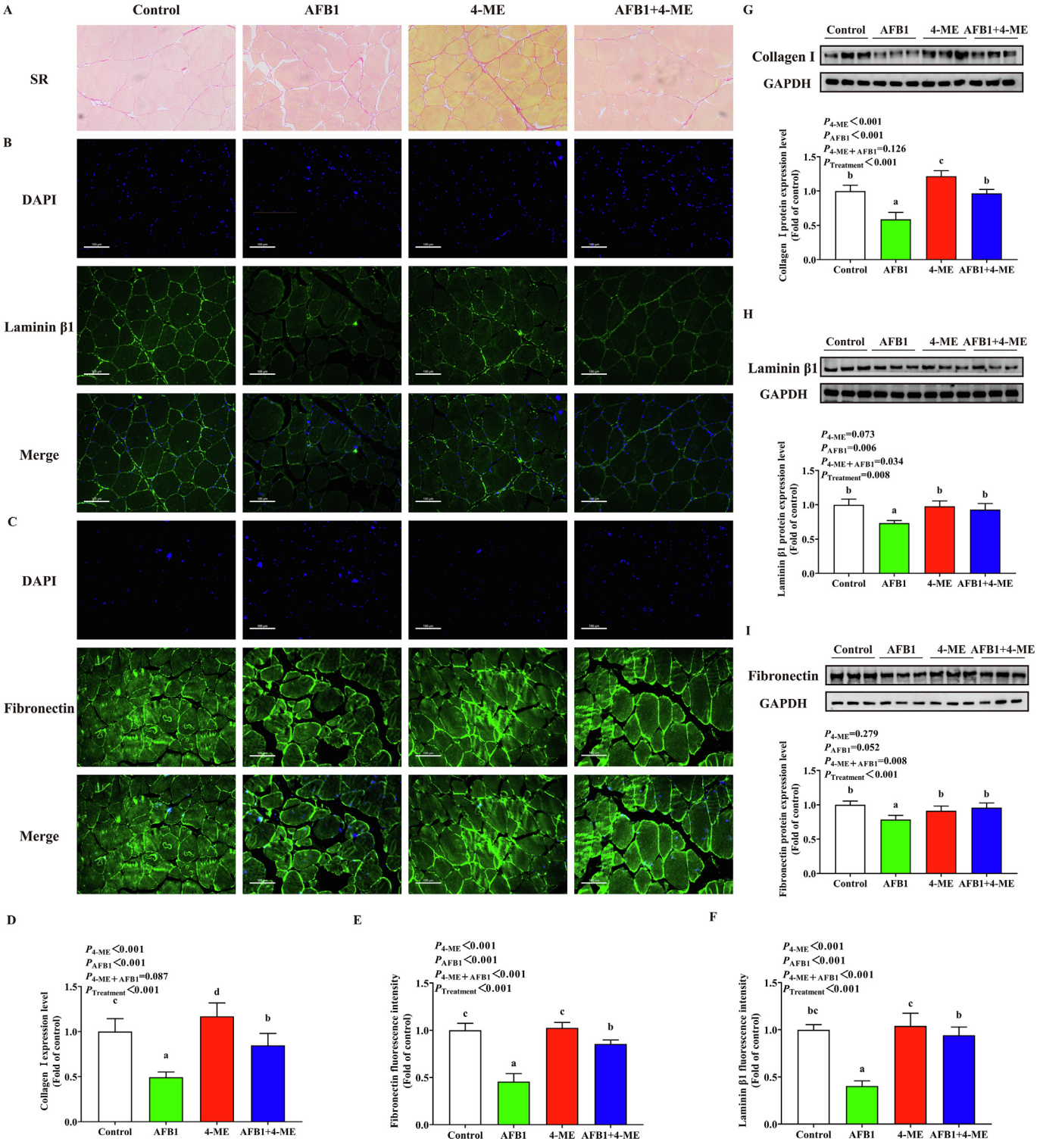

Fig. 3. 4-Methylesculetin (4-ME) alleviated the effects of aflatoxin B1 (AFB1) on the expression of extracellular matrix (ECM) main components in muscle of grass carp. (A) Representative images of collagen I distribution (200 ×). (B) Representative images of laminin β1 distribution (200 ×). (C) Representative images of fibronectin distribution (200 ×). (D) The quantification of staining collagen I with sirius red. (E) The quantification of laminin β1 fluorescence intensity. (F) The quantification of fibronectin fluorescence intensity. (G) The protein expression levels of collagen I. (H) The protein expression levels of laminin β1. (J) The protein expression levels of fibronectin. Control = control group, AFB1 = 60 μg/kg diet AFB1, 4-ME = 10 mg/kg diet 4-ME, AFB1+4-ME = 60 μg/kg diet AFB1 + 10 mg/kg diet 4-ME. $^{a\text{-}d}$ Different letters represent significant differences ($P < 0.05$). The data represent means ± SD. SR = sirius red; DAPI = 4',6-diamidino-2-phenylindole; GAPDH = glyceraldehyde-3- phosphate dehydrogenase.

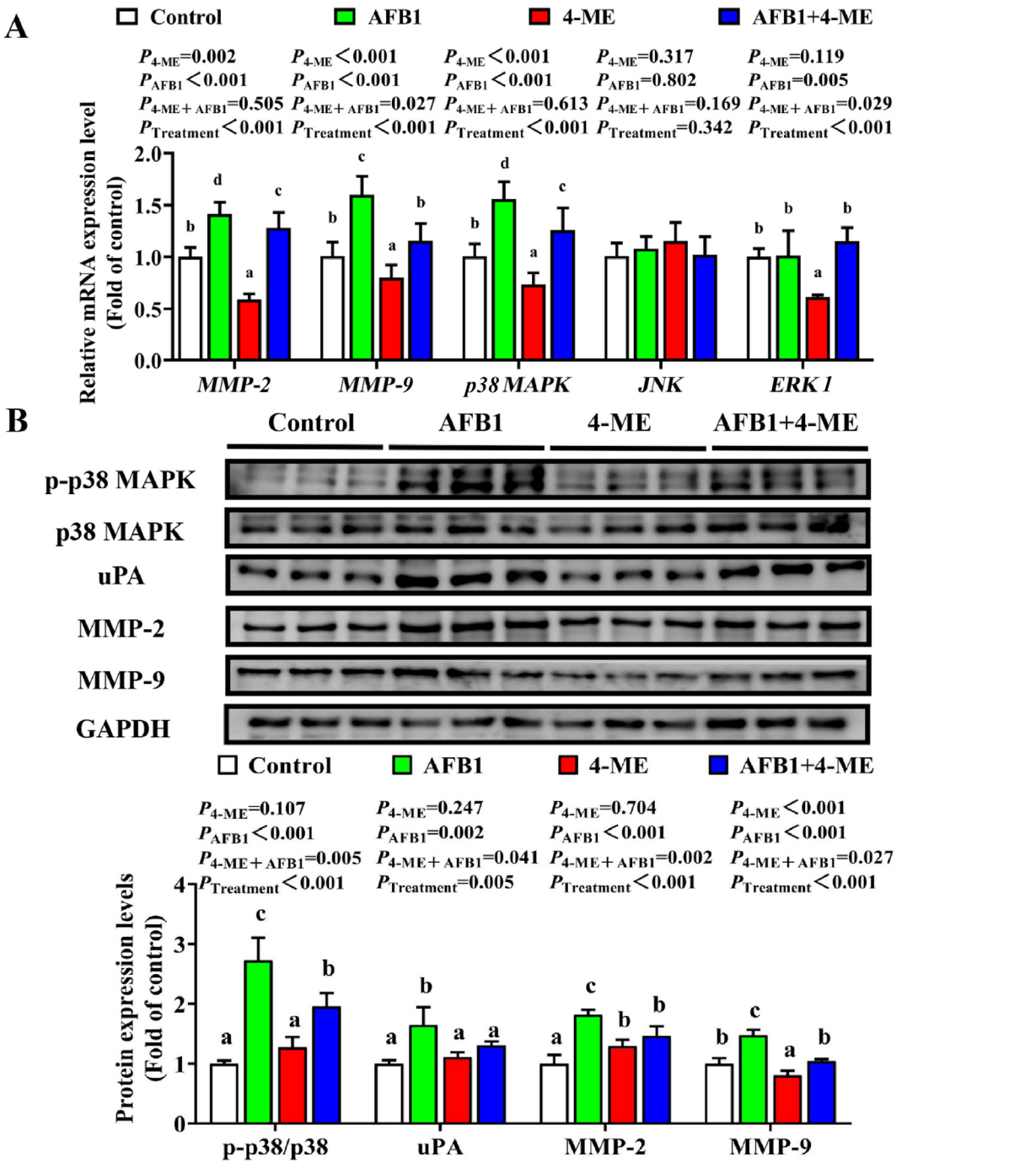

Fig. 4. 4-Methylesculetin (4-ME) alleviated the expression of aflatoxin B1 (AFB1)-induced extracellular matrix (ECM)-degrading enzymes and their regulatory signal molecules in grass carp muscle. (A) The relative mRNA expression levels of *MMP-2*, *MMP-9*, *p38 MAPK*, *JNK* and *ERK1*. (B) The protein expression levels of p-p38/p38 MAPK, uPA, MMP-2 and MMP-9. Control = control group, AFB1 = 60 μg/kg diet AFB1, 4-ME = 10 mg/kg diet 4-ME, AFB1+4-ME = 60 μg/kg diet AFB1 + 10 mg/kg diet 4-ME. [a-d] Different letters represent significant differences ($P < 0.05$). The data represent means ± SD. MMP-2 = matrix metalloproteinase-2; MMP-9 = matrix metalloproteinase-9; p38 MAPK = phosphorylate-38 mitogen-activated protein kinase; JNK = c-Jun N-terminal kinase; ERK1 = extracellular-signaling-related kinase 1; uPA = urokinase-type plasminogen activator; GAPDH = glyceraldehyde-3-phosphate dehydrogenase.

significantly improved the contents of MMP-2 and MMP-9 in myoblasts ($P < 0.05$), however, these MMP contents decreased following AFB1 + 4-ME treatment (Table 5) ($P < 0.05$). The relative mRNA expression results showed that AFB1 increased the transcriptional levels of *MMP-2* and *MMP-9* ($P < 0.05$), while AFB1 + 4-ME treatment down-regulated the transcriptional levels of these mRNA in myoblasts (Fig. 8A and B) ($P < 0.05$). Furthermore, the expression of uPA, MMP-2, MMP-9 and p-p38 MAPK proteins increased in AFB1 treatment ($P < 0.05$), while these proteins decreased following AFB1 + 4-ME treatment (Fig. 8C) ($P < 0.05$). Furthermore, the data revealed that SB203580 treatment decreased the protein expression levels of p-p38 MAPK, uPA, MMP-2, MMP-9 and improved the protein levels of collagen I, laminin β1 and fibronectin induced by AFB1 (Fig. 9A–G) ($P < 0.05$). These data

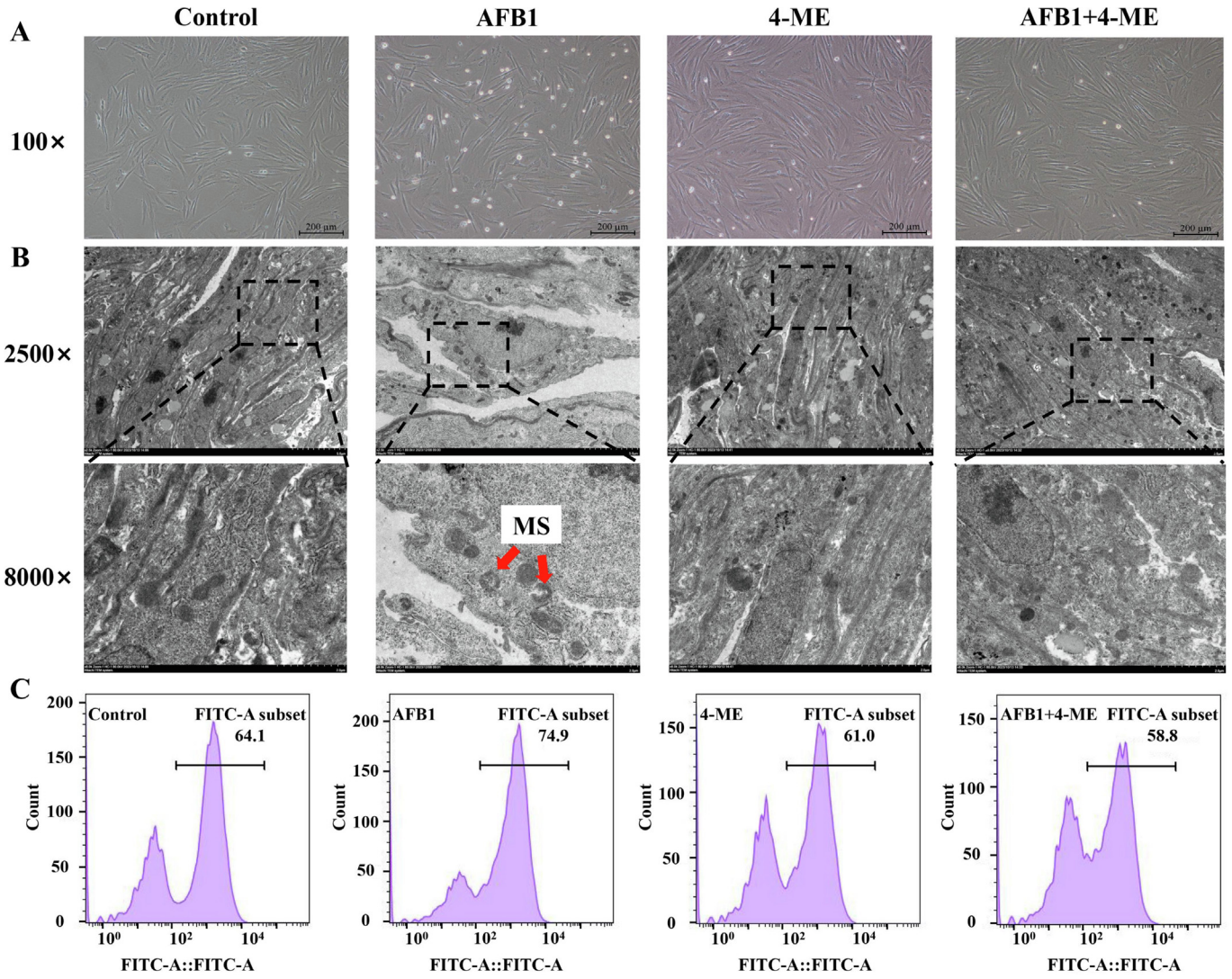

Fig. 5. 4-Methylesculetin (4-ME) alleviated the cell morphology and reactive oxygen species (ROS) levels of aflatoxin B1 (AFB1) on primary myoblasts of grass carp. (A) The images of representative cell morphology. (B) The cell ultrastructure representative images. (C) The ROS levels in the cells. Control = control group, AFB1 = 15 μmol/L AFB1, 4-ME = 0.5 μmol/L 4-ME, AFB1+4-ME = 15 μmol/L AFB1+0.5 μmol/L 4-ME. MS = mitochondrial swelling.

Table 4
4-ME alleviated the toxicity of AFB1 on primary myoblasts of grass carp (fold of control).

Item	Group[1]				*P*-value			
	Control	AFB1	4-ME	AFB1+4-ME	Treatment	4-ME	AFB1	AFB1+4-ME
ROS levels, %	100.00 ± 1.308^{c}	116.22 ± 1.065^{d}	88.59 ± 3.928^{a}	94.15 ± 4.748^{b}	<0.001	<0.001	<0.001	<0.001
Cell viability, %	100.00 ± 8.416^{c}	52.92 ± 5.385^{a}	96.28 ± 6.437^{c}	81.20 ± 7.367^{b}	<0.001	<0.001	<0.001	<0.001
LDH release, %	100.00 ± 4.108^{a}	189.31 ± 8.383^{c}	101.67 ± 5.347^{a}	160.143 ± 8.621^{b}	<0.001	<0.001	<0.001	<0.001

4-ME = 4-Methylesculetin; AFB1 = aflatoxin B1; ROS = reactive oxygen species; LDH = lactate dehydrogenase.
$^{a-c}$ Different letters represent significant differences ($P < 0.05$).
[1] Control = control group, AFB1 = 15 μmol/L AFB1, 4-ME = 0.5 μmol/L 4-ME = AFB1+4-ME = 15 μmol/L AFB1+0.5 μmol/L 4-ME. The data represent means ± SD.

indicated that 4-ME restrained p38 MAPK activation in grass carp primary myoblasts induced by AFB1.

4. Discussion

Fish skeletal muscles are the most abundant and edible parts and typically account for about 50% to 60% of the weight of the fish (Salem et al., 2018). It was reported that AFB1 caused oxidative damage and inhibited the muscle development of juvenile zebrafish (He et al., 2023a). Whether 4-ME could alleviate AFB1-induced oxidative damage and the inhibition of muscle development remains unclear. Grass carp is the most popular freshwater aquaculture species in China (Hu et al., 2019a). Our previous research results showed that 60 μg/kg AFB1 significantly reduced the growth performance and inhibited muscle development of grass carp (He et al., 2024b; Zeng et al., 2018). Based on these results, 60 μg/kg

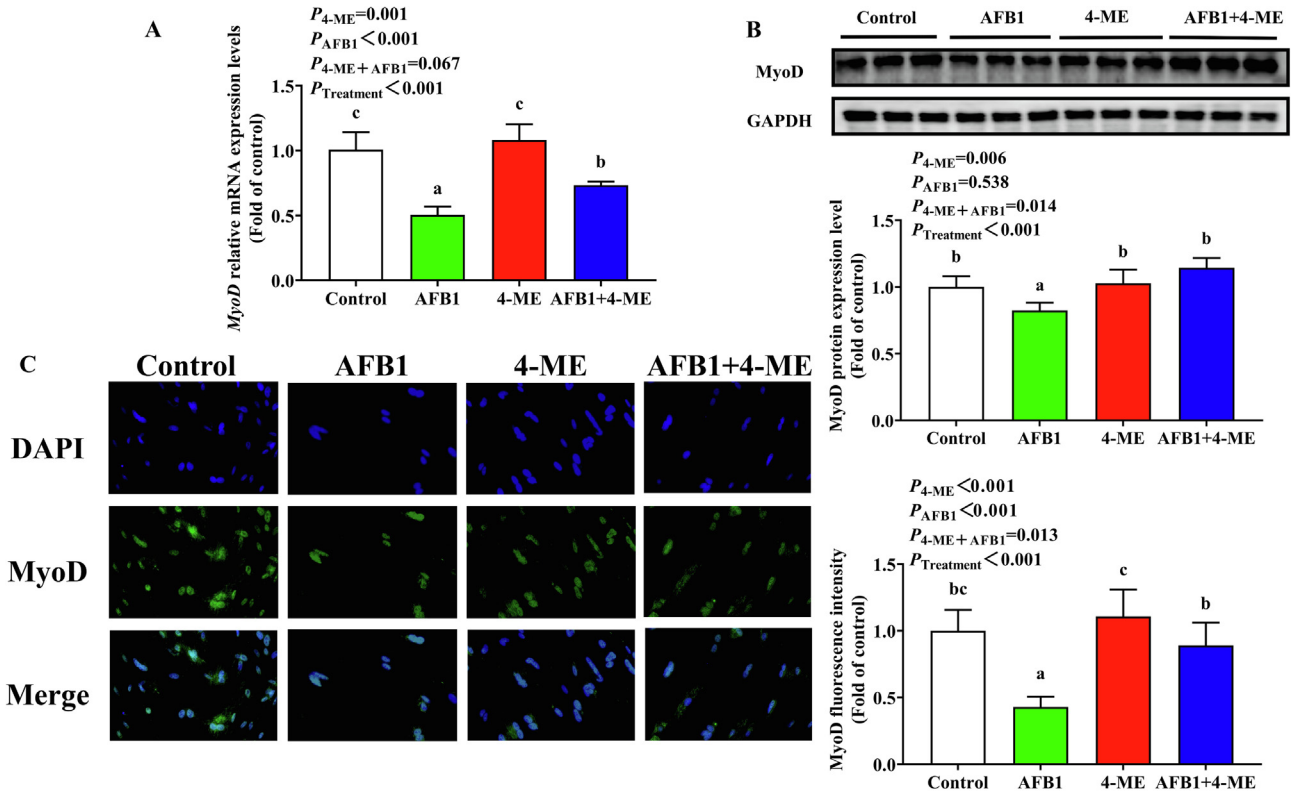

Fig. 6. 4-Methylesculetin (4-ME) alleviated the effects of aflatoxin B1 (AFB1) on the expression of myogenic differentiation (MyoD) in primary myoblasts of grass carp. (A) The relative mRNA expression levels of *MyoD*. (B) The protein expression levels of MyoD. (C) Representative images of MyoD distribution in cell (200 ×) and fluorescence intensity of MyoD protein expression levels. Control = control group, AFB1 = 15 μmol/L AFB1, 4-ME = 0.5 μmol/L 4-ME, AFB1+4-ME = 15 μmol/L AFB1+0.5 μmol/L 4-ME. $^{a\text{-}c}$ Different letters represent significant differences ($P < 0.05$). The data represent means ± SD. DAPI = 4',6-diamidino-2-phenylindole; GAPDH = glyceraldehyde-3-phosphate dehydrogenase.

AFB1 were selected. In the present research, grass carp and myoblast were used models to explore whether 4-ME could alleviate the inhibitory effect of AFB1 on fish growth and muscle development. It provided a theoretical basis for the safe development of the aquaculture industry. The data indicated that 4-ME effectively alleviated AFB1-induced inhibition of muscle development in grass carp mediated by the p38MAPK/uPA/MMP/ECM signaling pathway.

4.1. 4-ME alleviated AFB1-induced growth performance decline and muscle oxidative stress in grass carp

Mycotoxin contamination of food and feed is a global problem (Boonmee et al., 2020) and mycotoxin contamination of fish feed has caused a certain degree of threat to the development of the aquaculture industry. The data showed that AFB1 significantly reduced the growth performance (including SGR, PWG, FE, FI) of grass carp compared to the Control group, but 4-ME significantly alleviated them. A similar study on Nile tilapia found that AFB1 reduced the growth performance (Deng et al., 2010). The present study results showed that 4-ME alleviated the growth performance decline induced by AFB1.

ROS could cause the production of MDA in cell membranes, which may serve as a marker of tissue damage (Wardani et al., 2022). PC groups are fairly stable end products of protein oxidation by ROS (Dahiya et al., 2013). The level of PC is used to indicate protein oxidative damage, whereas the level of MDA indicates lipid oxidative damage (Lu et al., 2023). An important enzyme in redox signaling is GST (Matsui et al., 2020), reducing GST levels induces oxidative damage. The present study results found that AFB1 increased the levels of ROS (in vivo and in vitro), contents of MDA, PC and decreased the activity of GST in grass muscle suggesting that AFB1 caused muscle oxidative damage in grass carp. Furthermore, our previous study found that AFB1 caused oxidative damage by increasing MDA content and decreasing GST activity in zebrafish (He et al., 2023a). Studies on hybrid grouper (*Epinephelus fuscoguttatus*♀ × *Epinephelus lanceolatus*♂) have shown that AFB1 induced oxidative stress by increasing ROS levels in the liver (Liu et al., 2023). AFB1 also increased PC content in silver catfish (*Rhamdia quelen*) liver, and induced oxidative damage (de Freitas Souza et al., 2019). Natural products have good biological activities, including improving antioxidant capacity and immunity (Pyser et al., 2021) and are the main source of new chemical compounds that can be used in feed additives (Sukhikh et al., 2022). It was reported that 4-ME improved the antioxidant capacity by increasing the GST activity in rat colon (Tanimoto et al., 2020). In our results, supplementation with 4-ME could effectively alleviate the increase of ROS, PC and MDA levels, and the decrease of GST activity in grass carp muscle induced by AFB1, indicating that supplementation with 4-ME alleviated the oxidative damage induced by AFB1 in grass carp muscle.

4.2. 4-ME alleviated AFB1-induced destruction of muscle structure and inhibition of MRF expression in grass carp

Skeletal muscle constitutes 50% to 60% of fish body weight (Salem et al., 2018). Any changes in body weight are mainly reflected in changes in muscle growth and development. During

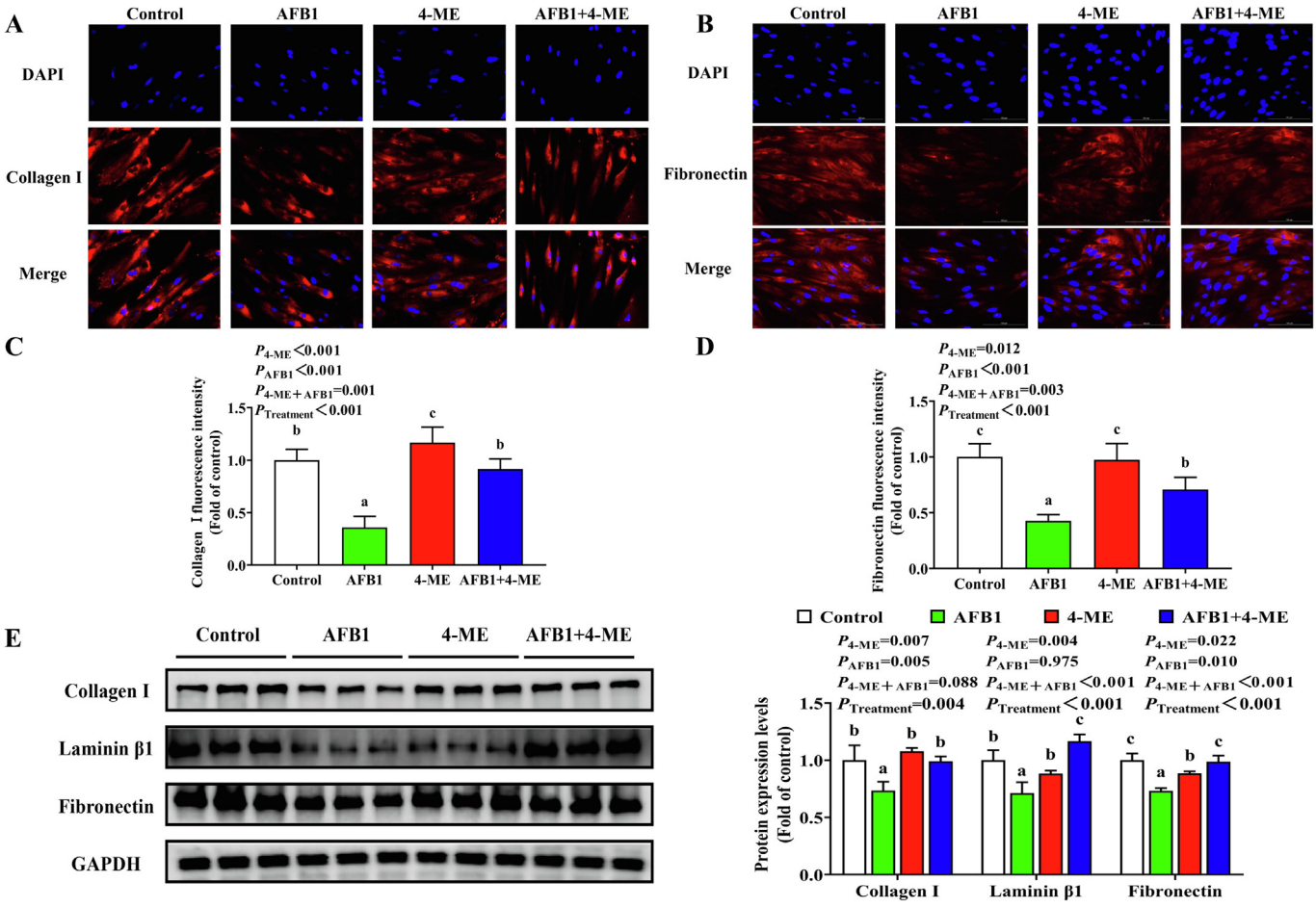

Fig. 7. 4-Methylesculetin (4-ME) alleviated the effects of aflatoxin B1 (AFB1) on the expression of extracellular matrix (ECM) main components in primary myoblasts of grass carp. (A) Representative images of collagen I distribution in cells (magnification 200×). (B) Representative images of fibronectin distribution in cells (magnification 200×). (C) The fluorescence intensity quantization results of collagen I. (D) The fluorescence intensity quantization results of fibronectin. (E) The protein expression levels of collagen I, laminin β1 and fibronectin in cells. Control = control group, AFB1 = 15 μmol/L AFB1, 4-ME = 0.5 μmol/L 4-ME, AFB1+4-ME = 15 μmol/L AFB1+0.5 μmol/L 4-ME. [a-c] Different letters represent significant differences ($P < 0.05$). The data represent means ± SD. DAPI = 4',6-diamidino-2-phenylindole; GAPDH = glyceraldehyde-3-phosphate dehydrogenase.

Table 5
4-ME alleviated the effects of AFB1 on the contents of MMP-2 and MMP-9 (ng/mL) in primary myoblasts of grass carp.

Item	Group[1]				*P*-value			
	Control	AFB1	4-ME	AFB1+4-ME	Treatment	4-ME	AFB1	AFB1+4-ME
MMP-2	882.01 ± 25.404[a]	985.11 ± 23.666[c]	916.99 ± 13.347[b]	913.07 ± 10.856[b]	<0.001	0.030	<0.001	<0.001
MMP-9	22.63 ± 4.221[a]	45.43 ± 5.390[c]	33.77 ± 5.199[b]	34.88 ± 4.380[b]	<0.001	0.883	<0.001	<0.001

4-ME = 4-Methylesculetin; AFB1 = aflatoxin B1; MMP-2 = matrix metalloproteinase-2; MMP-9 = matrix metalloproteinase-9.
[a-c] Different letters represent significant differences ($P < 0.05$).
[1] Control = control group, AFB1 = 15 μmol/L AFB1, 4-ME = 0.5 μmol/L 4-ME = AFB1 + 4-ME = 15 μmol/L AFB1 + 0.5 μmol/L 4-ME. The data represent means ± SD.

muscle development, myofibrils display periodic sarcomere patterns (Weitkunat et al., 2017). The results showed that AFB1 damaged the muscle ultrastructure in grass carp myofibrils, manifested as a disordered arrangement of myofibril and endoplasmic reticulum expansion. To our knowledge, there are no other studies that have investigated the effect of AFB1 on the ultrastructure of muscle. A study on another mycotoxin found that ochratoxin A (OTA) damaged the muscle histological structure and induced endoplasmic reticulum expansion in grass carp muscle (Zhao et al., 2023). The present study results suggested that AFB1 disrupted the histological structure of the muscle, which might inhibit muscle development. MyoD activates MyoG in developing muscle progenitors by acting as an early myogenic transcription factor (Cleveland et al., 2023). MyoD and MyoG have an important role in the differentiation of late myoblasts, causing myocytes to express structural proteins such as MYHC and differentiate into myotubes (Oliveira et al., 2022). As a major contractile protein of skeletal muscle cells, MYHC is responsible for muscle contractions (Wang et al., 2022), which is the most abundant muscle structural protein (Han et al., 2022). Our results

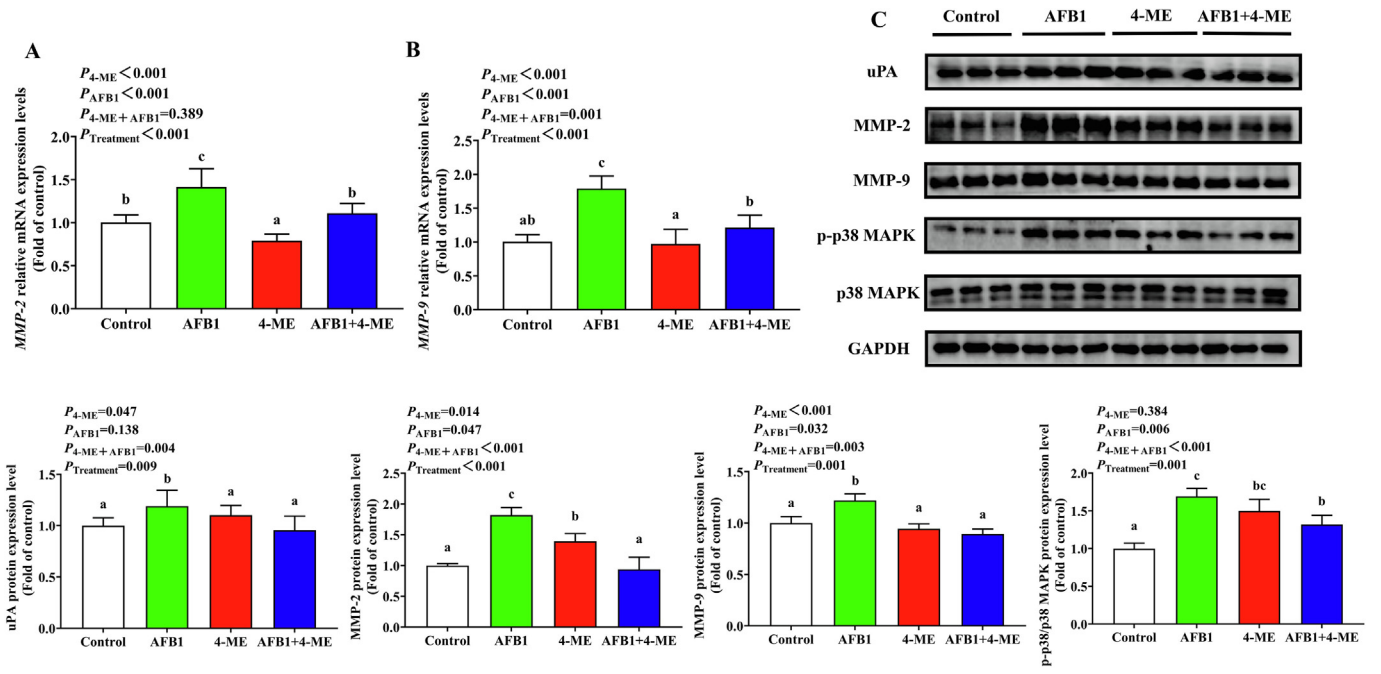

Fig. 8. 4-Methylesculetin (4-ME) alleviated the expression of aflatoxin B1 (AFB1)-induced extracellular matrix (ECM)-degrading enzymes and their regulatory signal molecules in primary myoblasts of grass carp. (A) The relative mRNA expression levels of *MMP-2*. (B) The relative expression mRNA levels of *MMP-9*. (C) The protein expression levels of uPA, MMPs, p-p38 MAPK and p38 MAPK. Control = control group, AFB1 = 15 μmol/L AFB1, 4-ME = 0.5 μmol/L 4-ME, AFB1+4-ME = 15 μmol/L AFB1+0.5 μmol/L 4-ME. [a-c] Different letters represent significant differences ($P < 0.05$). The data represent means ± SD. MMP-2 = matrix metalloproteinase-2; MMP-9 = matrix metalloproteinase-9; uPA = urokinase-type plasminogen activator; p38 MAPK = phosphorylate-38 mitogen-activated protein kinase; GAPDH = glyceraldehyde-3-phosphate dehydrogenase.

showed that AFB1 also inhibited muscle development of grass carp by down-regulating *MyoD* expression (in vivo and in vitro), *MyoG* and *MYHC* expression in grass carp muscle. A similar study found that AFB1 down-regulated the MRF (including *MyoG* and *MYHC*) mRNA expression in yellow catfish (Zhang et al., 2021b). A study of similar mycotoxins has found that OTA inhibited muscle development in grass carp by downregulating MRF gene expression (Zhao et al., 2023). Interestingly, in the present study, supplementation with 4-ME in grass carp diet promoted muscle development and alleviated the inhibition of muscle development induced by AFB1.

4.3. 4-ME alleviated the degradation of ECM in muscle induced by AFB1 in vivo and in vitro

ECM plays a crucial role in skeletal muscle development (Wang et al., 2020). The cleavage of MMP by uPA is essential for MMP activation, which could degrade ECM (Meng et al., 2018). MMP are proteolytic enzymes that degrade and remodel ECM in order to maintain the dynamic equilibrium of the ECM (Hu et al., 2020). In MDA-MB-231 cells, the overproduction of ROS could activate uPA (Flores-López et al., 2016). Our results showed that AFB1 induced ROS overproduction in grass carp muscle. Furthermore, AFB1 activated uPA, MMP-2, and MMP-9, in turn degrading laminin β1, collagen I and fibronectin in vivo and in vitro, while supplementation with 4-ME mitigated the degradation of ECM components. Similarly, 6,7-dihydroxycoumarin inhibited the production of pro-matrix metalloproteinase in rabbit articular chondrocytes (Watanabe et al., 1999). Therefore, we speculated that 4-ME might alleviate muscle development by alleviating oxidative damage and inhibiting the production of MMP induced by AFB1.

4.4. 4-ME alleviated AFB1-induced muscle development inhibition in vitro and in vivo through the p38MAPK signaling pathway

It was reported that the MAPK signaling pathway is known to regulate muscle atrophy, muscle satellite cell development (Segalés et al., 2016), and muscle structure in the Chronic Obstructive Pulmonary Disease mouse model (Mano et al., 2022). Furthermore, the expression of uPA and MMP was regulated by the MAPK signaling pathway in pancreatic cancer cells (Rachagani et al., 2012). MAPK signaling is mediated by three major molecules: p38 MAPK, ERK and JNK (Jung et al., 2020). The present findings suggested that AFB1 improved the expression of p38MAPK in vivo and in vitro, but ERK and JNK levels have not been changed, while 4-ME effectively alleviated the activation of p38MAPK induced by AFB1. A similar study found that AFB1 activated p38MAPK in grass carp gill (He et al., 2023b). In human gastric cancer SGC7901 cells, p38MAPK activation enhanced uPA, MMP-2, and MMP-9 expression (Lu et al., 2017). It is believed that MMP are involved in the degradation of proteins in the ECM (Ricci et al., 2014). ECM components (such as collagen, laminin, and fibronectin) could promote proliferation, differentiation, and migration in mice muscle cells (Goudenege et al., 2010; Liu et al., 2020). In addition, collagen I promotes the expression of MRF in mice (Goudenege et al., 2010; Liu et al., 2020). It was reported that coumarin derivatives inhibited p38MAPK activation in osteoclast (Abdallah et al., 2019). Therefore, we speculated that 4-ME might inhibit the degradation of ECM by

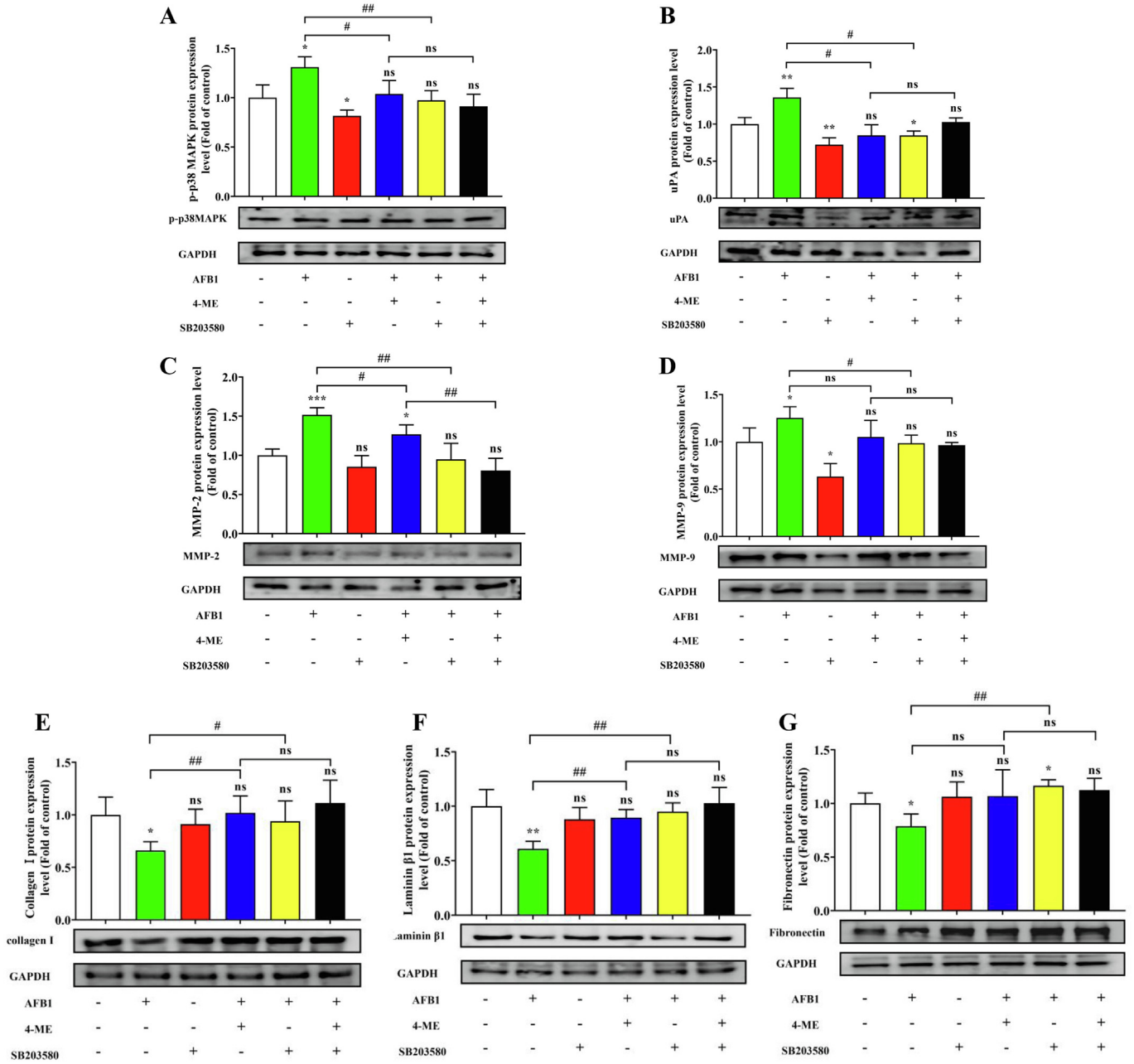

Fig. 9. Effects of 4-Methylesculetin (4-ME) and SB203580 on the protein levels of p38 MAPK signal molecules, extracellular matrix (ECM)-degrading enzymes and ECM main components in aflatoxin B1 (AFB1)-induced cells. (A) The protein expression levels of p-p38 MAPK and p38 MAPK. (B) The protein expression level of uPA. (C) The protein expression level of MMP-2. (D) The protein expression level of MMP-9. (E) The protein expression level of collagen I. (F) The protein expression level of laminin β1. (G) The protein expression level of fibronectin. Control = control group, AFB1 = 15 μmol/L AFB1, SB203580 = 10 mmol/L SB203580, AFB1+4-ME = 15 μmol/L AFB1+0.5 μmol/L 4-ME, AFB1+SB203580 = 15 μmol/L AFB1+10 mmol/L SB203580, AFB1+4-ME + SB203580 = 15 μmol/L AFB1+0.5 μmol/L 4-ME+10 mmol/L SB203580. + indicated added, - indicated not added. * Means compared to the control group, and # means compared to the AFB1 group or AFB1+4-ME group. * Indicates $P < 0.05$, ** indicates $P < 0.01$, and *** indicates $P < 0.001$, # indicates $P < 0.05$, ## indicates $P < 0.01$, ns indicated $P > 0.05$ (the difference is not significant). The data represent means ± SD. p38 MAPK = phosphorylate-38 mitogen-activated protein kinase; uPA = urokinase-type plasminogen activator; MMP-2 = matrix metalloproteinase-2; MMP-9 = matrix metalloproteinase-9; GAPDH = glyceraldehyde-3-phosphate dehydrogenase.

inhibiting the activation of p38MAPK induced by AFB1, thus alleviating muscle development.

5. Conclusion

To sum up, dietary AFB1 reduced the growth performance of grass carp, caused muscle oxidative damage, degraded ECM components by activating the p38MAPK pathway and inhibited muscle development. Dietary supplementation with 4-ME inhibited the activation of the p38MAPK pathway by alleviating oxidative damage induced by AFB1, thus alleviating muscle development. This study suggested that dietary 4-ME supplementation alleviated AFB1-induced muscle development inhibition in grass carp by the p38MAPK/uPA/MMP/ECM pathway. These findings could provide a theoretical basis for 4-ME as an animal feed additive to alleviate mycotoxins.

CRediT author statement

Xiangning He: Writing – Original draft, Investigation, Formal analysis. **Jiajia Zhang:** Writing – Original draft, Investigation, Formal analysis. **Weidan Jiang:** Resources. **Pei Wu:** Resources. **Yang Liu:** Validation. **Hongmei Ren:** Methodology. **Xiaowan Jin:** Methodology. **Hequn Shi:** Methodology. **Xiaoqiu Zhou:** Writing – Review & editing, Project administration, Conceptualization. **Lin Feng:** Writing – Review & editing, Project administration, Conceptualization.

Declaration of competing interest

We declare that we have no financial and personal relationships with other people or organizations that can inappropriately influence our work, and there is no professional or other personal interest of any nature or kind in any product, service and/or company that could be construed as influencing the content of this paper.

Acknowledgments

This research was financially supported by the National Natural Science Foundation of China (U23A20250), the earmarked fund for CARS (CARS-45), and the National Key R&D Program of China (2019YFD0900200). We would like to express our sincere thanks for the assistance from the personnel of the teams. We also thank the Home for Researchers (www.home-for-researchers.com).

Appendix A. Supplementary data

Supplementary data to this article can be found online at https://doi.org/10.1016/j.aninu.2024.08.001.

References

Abdallah BM, Ali EM, Elsawy H, Badr GM, Abdel-Moneim AM, Alzahrani AM. The coumarin derivative 5′-hydroxy auraptene suppresses osteoclast differentiation via inhibiting MAPK and c-Fos/NFATc1 pathways. BioMed Res Int 2019;2019(0):9395146.

Abdelhiee EY, Elbialy ZI, Saad AH, Dawood MA, Aboubakr M, El-Nagar SH, El-Diasty EM, Salah AS, Saad HM, Fadl SE. The impact of Moringa oleifera on the health status of Nile tilapia exposed to aflatoxicosis. Aquaculture 2021;533:736110.

Bailey EC, Alrowaished SS, Kilroy EA, Crooks ES, Drinkert DM, Karunasiri CM, Belanger JJ, Khalil A, Kelley JB, Henry CA. NAD+ improves neuromuscular development in a zebrafish model of FKRP-associated dystroglycanopathy. Skeletal Muscle 2019;9(1):1–23.

Boonmee S, Atanasova V, Chéreau S, Marchegay G, Hyde KD, Richard-Forget F. Efficiency of hydroxycinnamic phenolic acids to inhibit the production of ochratoxin A by Aspergillus westerdijkiae and Penicillium verrucosum. Int J Mol Sci 2020;21(22):8548.

Chen G, Cheng X, Shi G, Zou C, Chen L, Li J, Li M, Fang C, Li C. Transcriptome analysis reveals the effect of long intergenic noncoding RNAs on pig muscle growth and fat deposition. BioMed Res Int 2019;2019.

Chrouda A, Zinoubi K, Soltane R, Alzahrani N, Osman G, Al-Ghamdi YO, Qari S, Al Mahri A, Algethami FK, Majdoub H. An acetylcholinesterase inhibition-based biosensor for aflatoxin B1 detection using sodium alginate as an immobilization matrix. Toxins 2020;12(3):173.

Cleveland AH, Malawsky D, Churiwal M, Rodriguez C, Reed F, Schniederjan M, Velazquez Vega JE, Davis I, Gershon TR. PRC2 disruption in cerebellar progenitors produces cerebellar hypoplasia and aberrant myoid differentiation without blocking medulloblastoma growth. Acta Neuropathologica Communications 2023;11(1):8.

Dahiya P, Kamal R, Gupta R, Bhardwaj R, Chaudhary K, Kaur S. Reactive oxygen species in periodontitis. J Indian Soc Periodontol 2013;17(4):411.

de Freitas Souza C, Baldissera MD, Descovi S, Zeppenfeld C, Eslava-Mocha PR, Gloria EM, Zanette RA, Baldisserotto B, da Silva AS. Melaleuca alternifolia essential oil abrogates hepatic oxidative damage in silver catfish (*Rhamdia quelen*) fed with an aflatoxin-contaminated diet. Comp Biochem Physiol C Toxicol Pharmacol 2019;221:10–20.

Deng SX, Tian LX, Liu FJ, Jin SJ, Liang GY, Yang HJ, Du ZY, Liu YJ. Toxic effects and residue of aflatoxin B1 in tilapia (*Oreochromis niloticus*× *O. aureus*) during long-term dietary exposure. Aquaculture 2010;307(3–4):233–40.

Dong Y, Zhang X, Miao R, Cao W, Wei H, Jiang W, Gao R, Yang Y, Sun H, Qiu J. Branched-chain amino acids promotes the repair of exercise-induced muscle damage via enhancing macrophage polarization. Front Physiol 2022;13:2572.

El-Nezami H, Kankaanpää P, Salminen S, Ahokas J. Physicochemical alterations enhance the ability of dairy strains of lactic acid bacteria to remove aflatoxin from contaminated media. J Food Protect 1998;61(4):466–8.

Eshelli M, Harvey L, Edrada-Ebel R, McNeil B. Metabolomics of the bio-degradation process of aflatoxin B1 by actinomycetes at an initial pH of 6.0. Toxins 2015;7(2):439–56.

Flores-López LA, Martínez-Hernández MG, Viedma-Rodríguez R, Díaz-Flores M, Baiza-Gutman LA. High glucose and insulin enhance uPA expression, ROS formation and invasiveness in breast cancer-derived cells. Cell Oncol 2016;39:365–78.

Fux L, Ilan N, Sanderson RD, Vlodavsky I. Heparanase: busy at the cell surface. Trends Biochem Sci 2009;34(10):511–9.

Goudenege S, Lamarre Y, Dumont N, Rousseau J, Frenette J, Skuk D, Tremblay JP. Laminin-111: a potential therapeutic agent for Duchenne muscular dystrophy. Mol Ther 2010;18(12):2155–63.

Hah Y-S, Lee WK, Lee S, Seo J-H, Kim EJ, Choe Y-i, Kim SG, Yoo J-I. Coumestrol attenuates dexamethasone-induced muscle atrophy via AMPK-FOXO1/3 signaling. J Funct Foods 2023;100:105387.

Han YF, Guo WR, Su R, Zhang YN, Yang L, Borjigin G, Duan Y. Effects of sheep slaughter age on myogenic characteristics in skeletal muscle satellite cells. Animal Bioscience 2022;35(4):614.

Hassaan MS, Nssar KM, Mohammady EY, Amin A, Tayel SI, El-Haroun ER. Nano-zeolite efficiency to mitigate the aflatoxin B1 (AFB1) toxicity: effects on growth, digestive enzymes, antioxidant, DNA damage and bioaccumulation of AFB1 residues in Nile tilapia (*Oreochromis niloticus*). Aquaculture 2020;523:735123.

He XN, Jiang WD, Wu P, Liu Y, Ren HM, Jin XW, Kuang SY, Tang L, Li SW, Feng L. Aflatoxin B1 inhibited the development of primary myoblasts of grass carp (*Ctenopharyngodon idella*) by degrading extracellular matrix. Ecotoxicol Environ Saf 2024a;276:116332.

He XN, Wu P, Jiang WD, Liu Y, Kuang SY, Tang L, Ren HM, Li H, Feng L, Zhou XQ. Aflatoxin B1 exposure induced developmental toxicity and inhibited muscle development in zebrafish embryos and larvae. Sci Total Environ 2023a;878:163170.

He XN, Zeng ZZ, Feng L, Wu P, Jiang WD, Liu Y, Zhang L, Mi HF, Kuang SY, Tang L. Aflatoxin B1 damaged structural barrier through Keap1a/Nrf2/MLCK signaling pathways and immune barrier through NF-κB/TOR signaling pathways in gill of grass carp (*Ctenopharyngodon idella*). Aquat Toxicol 2023b;257:106424.

He XN, Zeng ZZ, Jiang WD, Wu P, Liu Y, Kuang SY, Tang L, Li SW, Feng L, Zhou XQ. Aflatoxin B1 decreased flesh flavor and inhibited muscle development in grass carp (*Ctenopharyngodon idella*). Animal Nutrition 2024b;18:27–38.

Hu Q, Xu S, Ye C, Jia J, Zhou L, Hu G. Novel pituitary actions of epidermal growth factor: receptor specificity and signal transduction for UTS1, EGR1, and MMP13 regulation by EGF. Int J Mol Sci 2019a;20(20):5172.

Hu TT, Yang JW, Yan Y, Chen YY, Xue HB, Xiang YQ, Ye LC. Detection of genes responsible for cetuximab sensitization in colorectal cancer cells using CRISPR-Cas9. Biosci Rep 2020;40(10):BSR20201125.

Hu W, Wang X, Bi Y, Bao J, Shang M, Zhang L. The molecular mechanism of the TEAD1 gene and miR-410-5p affect embryonic skeletal muscle development: a miRNA-mediated ceRNA network analysis. Cells 2023;12(6):943.

Hu X, Xing Y, Ren L, Wang Y, Li Q, Fu X, Yang Q, Xu L, Willems L, Li J. Bta-miR-24-3p controls the myogenic differentiation and proliferation of fetal bovine skeletal muscle-derived progenitor cells by targeting ACVR1B. Animals 2019b;9(11):859.

Jung HJ, Park SH, Cho KM, Jung KI, Cho D, Kim TS. Threonyl-tRNA synthetase promotes T helper type 1 cell responses by inducing dendritic cell maturation and IL-12 production via an NF-κB pathway. Front Immunol 2020;11:571959.

Kumar N, Dey CS. Metformin enhances insulin signalling in insulin-dependent and-independent pathways in insulin resistant muscle cells. Br J Pharmacol 2002;137(3):329–36.

Kwasek K, Choi YM, Wang H, Lee K, Reddish JM, Wick M. Proteomic profile and morphological characteristics of skeletal muscle from the fast-and slow-growing yellow perch (*Perca flavescens*). Sci Rep 2021;11(1):16272.

Lillehoj E, Stubblefield R, Shannon G, Shotwell O. Aflatoxin M1 removal from aqueous solutions by Flavobacterium aurantiacum. Mycopathologia 1971;45(3):259–66.

Liu H, Xie RT, Huang WB, Yang YZ, Zhou ML, Lu BQ, Li B, Tan BP, Dong XH. Negative effects of aflatoxin B1 (AFB1) in the diet on growth performance, protein and lipid metabolism, and liver health of juvenile hybrid grouper (*Epinephelus fuscoguttatus*♀× *Epinephelus lanceolatus*♂). Aquaculture Reports 2023;33:101779.

Liu X, Gao Y, Long X, Hayashi T, Mizuno K, Hattori S, Fujisaki H, Ogura T, Wang DO, Ikejima T. Type I collagen promotes the migration and myogenic differentiation of C2C12 myoblasts via the release of interleukin-6 mediated by FAK/NF-κB p65 activation. Food Funct 2020;11(1):328–38.

Lu SM, Zhang ZQ, Chen MR, Li CY, Liu LN, Li Y. Silibinin inhibits the migration and invasion of human gastric cancer SGC7901 cells by downregulating MMP-2 and MMP-9 expression via the p38MAPK signaling pathway. Oncol Lett 2017;14(6):7577–82.

Lu ZY, Feng L, Jiang WD, Wu P, Liu Y, Jiang J, Kuang SY, Tang L, Li SW, Zhong CB. Mannan oligosaccharides alleviate oxidative injury in the head kidney and spleen in grass carp (*Ctenopharyngodon idella*) via the Nrf 2 signaling

pathway after Aeromonas hydrophila infection. J Anim Sci Biotechnol 2023;14(1):1–15.
Mano Y, Tsukamoto M, Wang K-Y, Nabeshima T, Kosugi K, Tajima T, Yamanaka Y, Suzuki H, Kawasaki M, Nakamura E. Oxidative stress causes muscle structural alterations via p38 MAPK signaling in COPD mouse model. J Bone Miner Metabol 2022;40(6):927–39.
Matsui R, Ferran B, Oh A, Croteau D, Shao D, Han J, Pimentel DR, Bachschmid MM. Redox regulation via glutaredoxin-1 and protein S-glutathionylation. Antioxidants Redox Signal 2020;32(10):677–700.
Meng D, Lei M, Han Y, Zhao D, Zhang X, Yang Y, Liu R. MicroRNA-645 targets urokinase plasminogen activator and decreases the invasive growth of MDA-MB-231 triple-negative breast cancer cells. OncoTargets Ther 2018:7733–43.
Mousavi K, Zare H, Dell'Orso S, Grontved L, Gutierrez-Cruz G, Derfoul A, Hager GL, Sartorelli V. eRNAs promote transcription by establishing chromatin accessibility at defined genomic loci. Mol Cell 2013;51(5):606–17.
Oliveira TSd, Shimabukuro MK, Monteiro VRS, Andrade CBV, Boelen A, Wajner SM, Maia AL, Ortiga-Carvalho TM, Bloise FF. Low inflammatory stimulus increases D2 activity and modulates thyroid hormone metabolism during myogenesis in vitro. Metabolites 2022;12(5):416.
Pyser JB, Chakrabarty S, Romero EO, Narayan AR. State-of-the-art biocatalysis. ACS Cent Sci 2021;7(7):1105–16.
Rachagani S, Macha MA, Ponnusamy MP, Haridas D, Kaur S, Jain M, Batra SK. MUC4 potentiates invasion and metastasis of pancreatic cancer cells through stabilization of fibroblast growth factor receptor 1. Carcinogenesis 2012;33(10):1953–64.
Ricci C, Mota C, Moscato S, D'Alessandro D, Ugel S, Sartoris S, Bronte V, Boggi U, Campani D, Funel N. Interfacing polymeric scaffolds with primary pancreatic ductal adenocarcinoma cells to develop 3D cancer models. Biomatter 2014;4(1):e955386.
Salem M, Al-Tobasei R, Ali A, Lourenco D, Gao G, Palti Y, Kenney B, Leeds TD. Genome-wide association analysis with a 50K transcribed gene SNP-chip identifies QTL affecting muscle yield in rainbow trout. Front Genet 2018;9:387.
Segalés J, Perdiguero E, Muñoz-Cánoves P. Regulation of muscle stem cell functions: a focus on the p38 MAPK signaling pathway. Front Cell Dev Biol 2016;4:91.
Sukhikh S, Ivanova S, Babich O, Larina V, Krol O, Prosekov A, Popov A, Kriger O. Antimicrobial screening and fungicidal properties of Eucalýptus globulus ultrasonic extracts. Plants 2022;11(11):1441.
Tang M, Lu Y, Xiong Z, Chen M, Qin Y. The Grass Carp Genomic Visualization Database (GCGVD): an informational platform for genome biology of grass carp. Int J Biol Sci 2019;15(10):2119.
Tanimoto A, Witaicenis A, Caruso ÍP, Piva HM, Araujo GC, Moraes FR, Fossey MC, Cornélio ML, Souza FP, Di Stasi LC. 4-Methylesculetin, a natural coumarin with intestinal anti-inflammatory activity, elicits a glutathione antioxidant response by different mechanisms. Chem Biol Interact 2020;315:108876.
Tiago T, Hummel B, Morelli FF, Basile V, Vinet J, Galli V, Mediani L, Antoniani F, Pomella S, Cassandri M. Small heat-shock protein HSPB3 promotes myogenesis by regulating the lamin B receptor. Cell Death Dis 2021;12(5):452.
Wang SS, Tan BS, Xiao LY, Zhao XM, Zeng JK, Hong LJ, Yang J, Cai GY, Zheng EQ, Wu ZF. Comprehensive analysis of long noncoding RNA modified by m6A methylation in oxidative and glycolytic skeletal muscles. Int J Mol Sci 2022;23(9):4600.
Wang YX, Liu SY, Yan YQ, Li SF, Tong HL. SPARCL1 influences bovine skeletal muscle-derived satellite cell migration and differentiation through an ITGB1-mediated signaling pathway. Animals 2020;10(8):1361.
Wardani G, Nugraha J, Mustafa M, Kurnijasanti R, Sudjarwo SA. Antioxidative Stress and Antiapoptosis Effect of Chitosan nanoparticles to protect cardiac cell damage on streptozotocin-induced diabetic rat. Oxid Med Cell Longev 2022;2022.
Watanabe K, Ito A, Sato T, Saito T, Hayashi H, Niitani Y. Esculetin suppresses proteoglycan metabolism by inhibiting the production of matrix metalloproteinases in rabbit chondrocytes. Eur J Pharmacol 1999;370(3):297–305.
Weitkunat M, Brasse M, Bausch AR, Schnorrer F. Mechanical tension and spontaneous muscle twitching precede the formation of cross-striated muscle in vivo. Development 2017;144(7):1261–72.
Wilschut KJ, Haagsman HP, Roelen BA. Extracellular matrix components direct porcine muscle stem cell behavior. Exp Cell Res 2010;316(3):341–52.
Witaicenis A, de Oliveira ECS, Tanimoto A, Zorzella-Pezavento SFG, de Oliveira SL, Sartori A, Di Stasi LC. 4-methylesculetin, a coumarin derivative, ameliorates dextran sulfate sodium-induced intestinal inflammation. Chem Biol Interact 2018;280:59–63.
Yang GK, Liang XM, Hu JJ, Li CQ, Hu WP, Li KK, Chang XL, Zhang YM, Zhang XD, Shen YW. Feeding tea polysaccharides affects lipid metabolism, antioxidant capacity and immunity of common carp (*Cyprinus carpio L.*). Front Immunol 2022;13:1074198.
Ye SS, Mao BY, Yang L, Fu WY, Hou JR. Thrombosis recanalization by paeoniflorin through the upregulation of urokinase-type plasminogen activator via the MAPK signaling pathway. Mol Med Rep 2016;13(6):4593–8.
Yu Y, Shi J, Xie B, He Y, Qin Y, Wang D, Shi H, Ke Y, Sun Q. Detoxification of aflatoxin B1 in corn by chlorine dioxide gas. Food Chem 2020;328:127121.
Zamanian M, Hajizadeh M, Shamsizadeh A, Moemenzadeh M, Amirteimouri M, Elshiekh M, Allahtavakoli M. Effects of naringin on physical fatigue and serum MMP-9 concentration in female rats. Pharmaceut Biol 2017;55(1):423–7.
Zeng ZZ, Jiang WD, Wu P, Liu Y, Feng L. Dietary aflatoxin B1 decreases growth performance and damages the structural integrity of immune organs in juvenile grass carp (*Ctenopharyngodon idella*). Aquaculture 2018;500:1–17.
Zhang W, Liu Y, Zhang H. Extracellular matrix: an important regulator of cell functions and skeletal muscle development. Cell Biosci 2021a;11:1–13.
Zhang ZY, Jiang ZY, Lv HB, Jin JY, Chen LQ, Zhang ML, Du ZY, Qiao F. Dietary aflatoxin impairs flesh quality through reducing nutritional value and changing myofiber characteristics in yellow catfish (*Pelteobagrus fulvidraco*). Anim Feed Sci Technol 2021b;274:114764.
Zhao P, Liu X, Feng L, Jiang WD, Wu P, Liu Y, Ren HM, Jin XW, Yang J, Zhou XQ. New perspective on mechanism in muscle toxicity of ochratoxin A: model of juvenile grass carp (*Ctenopharyngodon idella*). Aquat Toxicol 2023;263:106701.